NOAA Technical Memorandum ERL GLERL-70

LUMPED MODELING OF LAURENTIAN GREAT LAKES EVAPORATION, HEAT STORAGE, AND ENERGY FLUXES FOR FORECASTING AND SIMULATION

Thomas E. Croley II

Great Lakes Environmental Research Laboratory
Ann Arbor, Michigan
February 1989

UNITED STATES DEPARTMENT OF COMMERCE

Robert A. Mosbacher
Secretary

NATIONAL OCEANIC AND ATMOSPHERIC ADMINISTRATION

William E. Evans
Under Secretary for Oceans and Atmosphere/Administrator

Environmental Research Laboratories

Joseph 0. Fletcher
Director

NOTICE

Mention of a commercial company or product does not constitute an endorsement by NOAA Environmental Research Laboratories. Use for publicity or advertising purposes of information from this publication concerning proprietary products or the tests of such products is not authorized.

For sale by the National Technical Information Service, 5285 Port Royal Road
Springfield, VA 22161

CONTENTS

FIGURES

TABLES

Page

LUMPED MODELING OF LAURENTIAN GREAT LAKES EVAPORATION, HEAT STORAGE, AND ENERGY FLUXES FOR FORECASTING AND SIMULATION*

Thomas E. Croley, II

ABSTRACT. Lake evaporation for the Laurentian Great Lakes is of the same order of magnitude as precipitation and runoff to the lakes and its estimation is important for simulations and forecasts of lake levels. Water or energy balance estimates of Great Lakes evaporation require storage-change data, not available in simulations or forecasts, and errors in the components of the balances are summed in the residual, giving large estimation errors for evaporation. Evaporation models, which use the aerodynamic equation with mass transfer coefficients developed originally in the Lake Hefner studies, were further developed for Lake Ontario during the International Field Year for the Great Lakes and adapted for other Great Lakes. Neither these models nor the balance models can be verified since independent estimates of evaporation are not available with sufficient accuracy. However, surface temperatures are available and **can** be used as verification data. The mass transfer coefficient research (where water surface temperatures must be known) is combined here with lumped model concepts of classical energy conservation and superposition heat storage to provide continuous simulation capability of both water surface temperatures and lake evaporation for use in outlooks and forecasts of lake levels. A new function is presented that uses a simple relation between surface temperature and heat stored in a lake based on current understandings of the thermal structure of large lakes. Calibration of the resulting model matches the water surface temperatures for those Great Lakes and small Lake St. Clair with satellite observations of water surface temperatures over the past 20 years. Evaporation and heat budgets over the annual cycle are presented for four of the Great Lakes and Lake St. Clair, and comparisons with long-term water balances are made.

1. INTRODUCTION

Understanding short- and long-term variations in the Laurentian Great Lakes water levels and the hazards associated with them requires lake-level forecasts and simulations, both of which have lake evaporation modeling as an integral part. Because lake evaporation for the Great Lakes is on the same order of magnitude as precipitation and runoff to the lakes, it represents a significant component of the Great Lakes hydrologic cycle and its determination is crucial in estimating lake levels. Evaporation determination for large lakes is still difficult even after years of research owing to the unavailability of pertinent data over large areas, the complexity of the evaporation process, and **the** present lack of understanding of heat storage in large lakes. The Great Lakes Environmental Research Laboratory has been using evaporation work developed during the International Field Year for the Great Lakes (IFYGL) for Lake Ontario modified for other lakes; that work uses the aerodynamic equation with mass transfer coefficients developed originally in the Lake Hefner studies of the late 1940's and early 1950's to estimate monthly evaporation from monthly data. Unfortunately, there have been no really good independent evaporation data to verify this approach on the Great Lakes. Water balance determinations (Bennett, 1978a) are insufficient, owing to **the** large errors introduced by subtracting nearly equal large inflows and outflows to each Great Lake except Superior. Even for Lake Superior, with its relatively smaller inflows and outflows, **the** water balance allows only a crude comparison. Energy balances (Bennett, 1978b; Bolsenga, 1975; Schertzer, 1978, 1987) also suffer by summing errors in all terms into the residual evaporation **estimate.**

[1]GLERL Contribution No. 633

Since uses of the aerodynamic equation and of energy balance techniques require knowledge of surface temperatures, a second problem is that they are not amenable to use in forecast settings (where future surface temperatures are unknown). It is necessary to model both the heat storage and the evaporation process (through consideration of the heat balance and surface temperature) to enable extrapolation of surface temperatures for forecasting evaporation. Until recently, such consideration was not possible because Great Lake surface temperatures have not been widely available for calibration of such a model. Now, remotely-sensed (satellite) historical surface temperatures are available for all Great Lakes except Michigan; they form an independent set of data that may be used for comparisons in evaporation heat balance calculations and model verification.

To take advantage of the newly available surface temperature data, to allow recognition of meteorological variability filtered by monthly averaging, and to remain consistent with other Great Lakes hydrology models, a daily evaporation model is desired for use over the lake surface. To avoid an additional computational burden inappropriate for long simulations, calibrations, or real-time forecasts, and to maintain model sophistication in line with data availability, a spatially-lumped model of the entire lake surface is constructed. As a first effort, concepts of heat storage are combined here with lumped or zero-dimension models of the heat balance and evaporation process to estimate Great Lakes evaporation efficiently in simulation and forecast settings. Existing work is used on Great Lakes evaporation modeling (where water temperatures must be known) and classical energy conservation; a simple relation between surface temperatures and heat storage in a lake is investigated based on current understandings of the thermal structure of a large lake. These concepts are combined and the resulting model is calibrated with surface temperatures for four of the Great Lakes and Lake St. Clair and compared with existing evaporation estimates.

2. GREAT LAKES EVAPORATION MODEL

Great Lakes evaporation studies have typically used mass transfer formulations from the classic Lake Hefner study (U.S. Geological Survey, 1954, 1958); see Richards and Irbe (1969) and Derecki (1976a). More recently, Phillips (1978) and Quinn (1979) included atmospheric stability effects on Great Lakes evaporation bulk transfer coefficients; the latter approach is used now by both Canadian and U.S. agencies, applied to monthly data for surface temperatures, wind speed, humidity, and air temperatures (Derecki, 1976a,b, 1979, 1981a,b; Quinn and Kelley, 1983; Atmospheric Environment Service, 1988). The present study uses that approach and it is outlined here for convenience (after [Quinn, 19791).

2.1 Bulk Evaporation Coefficient

Paulson (1970) summarized the application of Monin and Obukhov's similarity hypothesis to field measurements of wind speed and air temperature in the atmospheric surface layer (in which turbulent fluxes are taken as constant with height). Following Panofsky (1963) and Businger (1966), he established wind and temperature profiles respectively as

$$U = U_* k^{-1} [\ln(Z / Z_w) - S_1] \quad (1)$$

and

$$T - T_w = T_* [\ln(Z / Z_w) - S_2] \quad (2)$$

where U = mean wind speed at reference height Z above the surface, U_* = friction velocity, k = von Kármán's constant, Z_w = roughness length, T = potential temperature at reference height, T_w = potential temperature at Z_w, and

$$T_* = -Q / (r C_p k U_*) \quad (3)$$

$$S_1 = 2\ln\{[1 + (1 - a_1 Z / L)^{1/4}] / 2)$$

$$+ \ln\{[1 + (1 - a_1 Z / L)^{1/2}] / 2)$$

$$- 2\tan^{-1}(1 - a_1 Z / L)^{1/4} + 1.5707\% \quad , Z / L \leq 0 \qquad (4)$$

$$= -a_2 Z / L \quad , 0 < Z / L < 1$$

$$= -a_2 (1 + \ln(Z / L)] \quad , Z / L \geq 1$$

$$S_2 = 2\ln\{[1 + (1 - a_3 Z / L)^{1/2}] / 2) \quad , Z / L \leq 0$$

$$= -a_2 Z / L \quad , 0 < Z / L < 1 \qquad (5)$$

$$= -a_2 [1 + \ln(Z / L)] \quad , Z / L \geq 1$$

where T_* = a scaling temperature, Q = turbulent heat flux, r = air density, C_p = specific heat of air at constant temperature, Sl and S2 = stability-dependent parameters for the wind and temperature profiles respectively, and

$$L = -U_*^3 C_p r \Upsilon / (k g Q) \qquad (6)$$

where L = Monin-Obukhov length, Υ = absolute temperature of near-surface air, and g = acceleration due to gravity. Note from (4) and (5) that wind speed and air temperature are functions of the stability parameter, Z / L, where Z / L < 0 denotes unstable conditions, Z / L = 0 is neutral, 0 < Z / L < 1 is stable, and Z / L $\geq$ 1 is strongly stable.

Quinn (1979) used Charnock's (1955) relationship for neutral conditions over a large surface to obtain

$$Z_w = a_4 U_*^2 / g . \qquad (7)$$

By taking the bulk evaporation coefficient C_E equal to the sensible heat coefficient C_H Quinn (1979) used the following expression for turbulent heat flux,

$$Q = -r C_p C_H (T - T_w) U , \qquad (8)$$

and (1), (2), and (3) to get

$$C_E = k U_* U^{-1} [\ln(Z / Z_w) - S_2]^{-1} . \qquad (9)$$

As a result, evaporation over water E_w can be expressed as an equivalent depth by the bulk aerodynamic evaporation formulation

$$E_w = r C_E (q_w - q) U / r_w \qquad (10)$$

where q = specific humidity of the atmosphere, q_w = saturation specific humidity at the surface temperature, and r_w = density of water.

By combining (1), (2), and (3) with (6), we have

$$L = U^2 \Upsilon g^{-1} (T - T_w)^{-1} [\ln(Z / Z_w) - S_2] [\ln(Z / Z_w) - S_1]^{-2} . \qquad (11)$$

Equations (1), (4), (5), (7), (9), (10), and (11) were solved by Quinn (1979) for his computations of over-lake evaporation on Lake Ontario with data taken during IFYGL; he used daily and monthly observations of over-water wind speed (U) and air-water temperature difference (taken as $T - T_w$) with an iterative simultaneous solution. Initially, $U_* = 0.1$ m s^{-1}, $S_1 = 0$, and S2 = 0 are assumed, Z_w and L are computed from (7) and (11) respectively, and S_1, S2, U_*, Z_w, and L are recomputed from (4), (5), (1), (7), and (11) respectively; the last step is repeated to converge on the solution. Finally, CE is determined by (9). Quinn chose empirical coefficients al = 16 (Paulson, 1970), a2 = 5.2 (Webb, 1970), a_3 = 16 (Dyer, 1974), and k = 0.41 (Hicks, 1976) as best representing the atmospheric surface layer and determined a4 = 0.0101 by using Smith and Banke's (1975) findings with observations of his own. He also used Z = 8 m, g = 9.8 m s^{-2}, and constant Υ = 276.5 kelvins (K), since normal variations in Υ make little difference in L.

2.2 Over-Water Meteorology

Because over-water data are not available generally, over-land data are used with correction for over-water conditions. Data on air temperatures, wind speed, humidity, and cloud cover were taken from selected stations about each lake (Fig. 1; Table 1) and averaged for each lake to determine over-land meteorology to which over-water corrections can be applied. The stations were chosen to give an areally balanced distribution about each lake with as complete a record as possible for the period 1948-85, representing at least five stations. Hourly meteorology was obtained from the Atmospheric Environment Service (AES) for Canadian stations and from the National Climatic Data Center (NCDC) for U. S. stations. Hourly wind speeds, air temperatures, and cloud cover were averaged to obtain daily estimates.

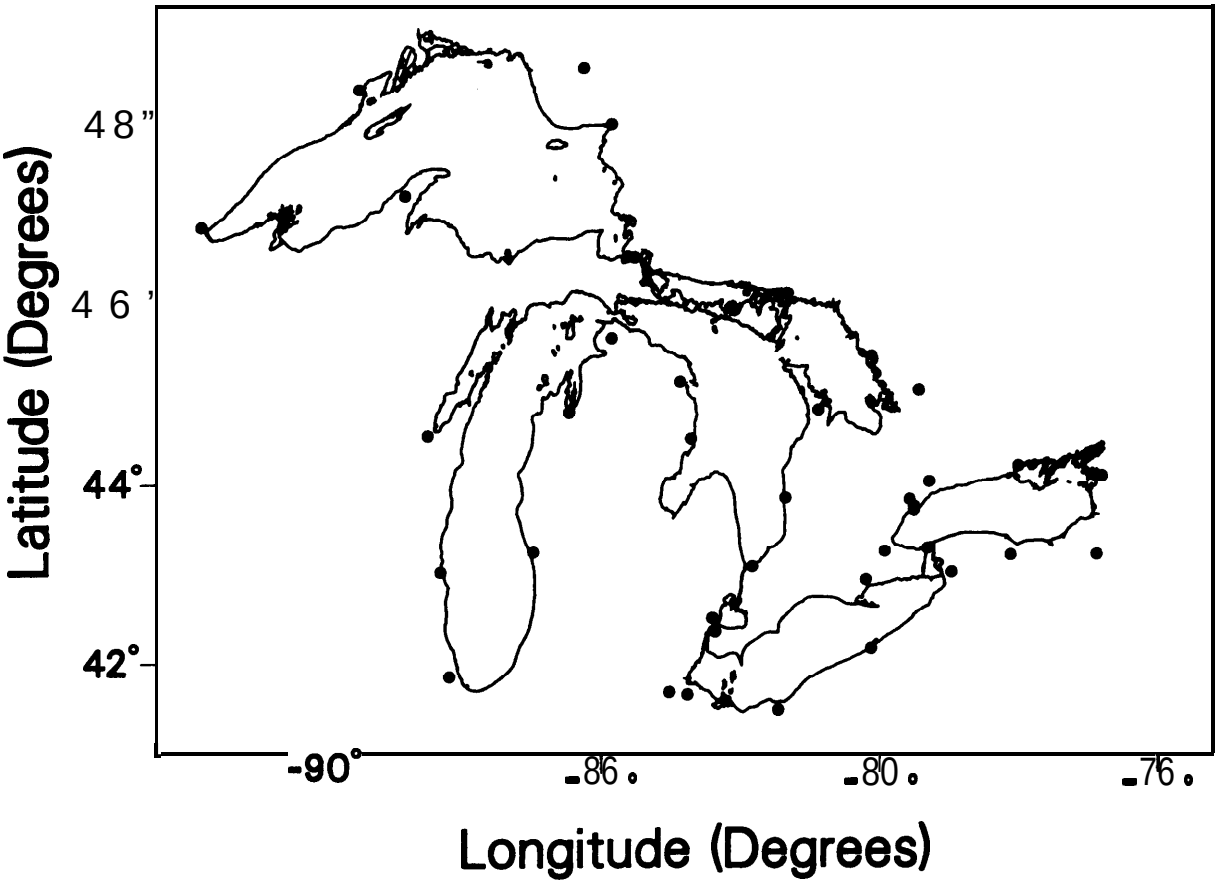

Figure l.--Locations of Great Lakes over-land meteorology stations.

Table 1.--Over-land meteorology stations used about each Great Lake

Station Name[a]	Number[b]	Lat.	Long.	Period of Record
		LAKE SUPERIOR		
Duluth, MN	14913	46.83	-92.18	01/01/48 - 31/12/85
Sault Ste. Marie, MI	14847	46.47	-84.37	01/01/48 - 31/12/85
Houghton, MI	14858	47.17	-88.50	01/01/48 - 31/12/85
Sault Ste. Marie A, ONT	6057592	46.48	-84.50	01/08/61 - 31 /01/87
Wawa A, ONT	6059D09	47.97	-84.78	01/01/77 - 31/01/87
White River, ONT	6059475	48.60	-85.28	01/01/53 - 31/02/76
Thunder Bay A, ONT	6048261	48.37	-89.32	01/01/53 - 31/01/87
		LAKE MICHIGAN		
Traverse City, MI	14850	44.73	-85.58	01/12/48 - 31/12/85
Muskegon, MI	14840	43.17	-86.23	01/01/48 - 31/12/85
Chicago, IL	14819	41.78	-87.75	01/01/48 - 31/12/79
Milwaukee, WI	14839	42.95	-87.90	01/01/48 - 31/12/85
Green Bay, WI	14898	44.48	-88.13	01/09/49 - 31/12/85
		LAKE HURON		
Alpena, MI	94849	45.07	-83.57	01/09/59 - 31/12/85
Pellston, MI	14841	45.57	-84.80	01/01/48 - 31/12/54
Oscoda, MI	14808	44.43	-83.38	01/11/50 - 31/12/70
Gore Bay A, ONT	6092925	45.88	-82.57	01/01/53 - 31/01/87
Muskoka A, ONT	6115525	44.97	-79.30	01/01/53 - 31/01/87
Wiarton A, ONT	6119500	44.75	-81.10	01/01/53 - 31/01/87
Goderich Municipal A, ONT	6122849	43.77	-81.70	03/11/69 - 31/10/80
Sarnia A, ONT	6127514	43.00	-82.30	01/12/67 - 31/01/87
		LAKE ST. CLAIR		
Detroit, MI	14822	42.42	-83.02	01/01/48 - 31/12/85
Windsor A, ONT	6139525	42.27	-82.97	01/01/53 - 31/01/87
		LAKE ERIE		
Toledo, OH	14849	41.57	-83.47	01/01/46 - 31/01/55
Toledo, OH	94830	41.60	-83.80	01/02/55 - 31/12/82
Cleveland, OH	14820	41.40	-81.85	01/01/48 - 31/12/82
Erie, PA	14860	42.08	-80.18	01/01/48 - 31/12/82
Buffalo, NY	14733	42.93	-78.73	01/01/48 - 31/12/82
Windsor A, ONT	6139525	42.27	-82.97	01/01/53 - 31/01/87
Simcoe, ONT	6137730	42.85	-80.27	01/01/62 - 31/12/86
		LAKE ONTARIO		
Rochester, NY	14768	43.12	-77.67	01/01/48 - 31/12/85
Syracuse, NY	14771	43.12	-76.12	01/01/45 - 31/12/82
Watertown, NY	94790	44.00	-76.02	01/05/49 - 31/12/64
St Catharines A, ONT	6137287	43.20	-79.17	01/06/71 - 31 /01/87
Hamilton A, ONT	6153194	43.17	-79.93	01/01/70 - 31/01/87
Toronto, ONT	6158350	43.67	-79.40	01 /01/53 - 01/05/69
Toronto Downsview A, ONT	6158443	43.75	-79.48	01/10/56 - 01/06/82
Toronto Island A, ONT	6158665	43.63	-79.40	01/02/57 - 31/01/87
Toronto New Int'l A, ONT	6158749	43.95	-79.13	01/06/73 - 01/03/76
Trenton A, ONT	6158875	44.12	-77.53	01/01/53 - 31/01/87

[a] Airport stations are designated by A.
[b] Five-digit numbers are U.S. stations from the National Climate Data Center; seven digits are Canadian stations from the Atmospheric Environment Service.

The AES supplied hourly relative humidities and the NCDC provided hourly dew point temperatures: The AES hourly humidities were averaged over the day and used with daily air temperatures to compute the daily dew point temperature. To be consistent, the NCDC hourly dew point temperatures were converted to hourly relative humidities, which were then averaged and used with daily air temperatures to compute the daily dew point temperature.

Derecki applied Quinn's approach to Lakes Superior, St. Clair, and Erie (Derecki, 1976a,b, 1979, 1981a,b), by adjusting for over-water conditions on the basis of Phillips and Irbe's (1978) studies of over-water data available from specially placed data buoys on Lake Ontario during IFYGL. In stepwise multiple linear regressions, Phillips and Irbe related over-water data to air stability (indexed by the over-land air temperature minus the surface temperature), fetch length in the wind direction, over-land wind speed, duration of air over water, over-land air temperature, surface temperature, and over-land dew point temperature. because some of these variables are not generally available, Derecki used Phillips and Irbe's data for over-water corrections by replacing the fetch (and derived quantities) with averages over the data set for each stability class and by fitting fifth-order polynomials to the corrections as a function of stability. The resulting equations give poor results outside the range of the data they were based on. Here, Phillips and Irbe's original regressions for over-water corrections are used directly by replacing the fetch (and derived quantities) with averages over the data set for each stability class. The results are then used for all lakes (except for Lake St. Clair) although derived originally for Lake Ontario, in a manner similar to Derecki's efforts; for Lake St. Clair, a fetch of 10.5 nautical miles is used in place of the average over the data set since Lake St. Clair is so much smaller than the Great Lakes. The following apply to all lakes except Lake St. Clair:

$$
\begin{aligned}
U &= 3.132 + 1.05\ W && , T_a - T_w \le -10.5 \\
&= 2.795 + 1.01\ w && , -10.5 < T_a - T_w \le -3.5 \\
&= 1.607 + 0.92\ W - 0.28\ (T_a - T_w) && , -3.5 < T_a - T_w \le 3.5 \\
&= 2.740 + 0.49\ W - 0.02\ T_a && , 3.5 < T_a - T_w \le 10.5 \\
&= 3.374 + 0.32\ W - 0.02\ T_a && , T_a - T_w > 10.5
\end{aligned}
\qquad (12)
$$

$$
\begin{aligned}
T &= -1.333 + 0.60\ T_a + 0.54\ T_w && , T_a - T_w \le -10.5 \\
&= -0.321 + 0.67\ T_a + 0.42\ T_w && , -10.5 < T_a - T_w \le -3.5 \\
&= 0.290 + 0.47\ T_a + 0.52\ T_w && , -3.5 < T_a - T_w \le 3.5 \\
&= 1.485 + 0.29\ T_a + 0.65\ T_w && , 3.5 < T_a - T_w \le 10.5 \\
&= 1.822 + 0.30\ T_a + 0.56\ T_w && , T_a - T_w > 10.5
\end{aligned}
\qquad (13)
$$

$$
\begin{aligned}
D &= -4.499 + 0.56\ D_l + 0.46\ T_w && , T_a - T_w \le -10.5 \\
&= 0.484 + 0.94\ D_l + 0.11\ T_w && , -10.5 < T_a - T_w \le -3.5 \\
&= -0.350 + 0.72\ D_l + 0.31\ T_w && , -3.5 < Ta - Tw \le 3.5 \\
&= -0.160 + 0.44\ D_l + 0.55\ T_w && , 3.5 < T_a - T_w \le 10.5 \\
&= -0.037 + 0.43\ D_l + 0.53\ T_w && , T_a - T_w > 10.5
\end{aligned}
\qquad (14)
$$

where U is expressed in meters per second, W = over-land wind speed ($m s^{-1}$), T_a = over-land air temperature (°C), T_w and T are expressed in degrees Celsius, D = over-water dew point temperature (°C), and D_l = over-land dew point temperature (°C). For Lake St. Clair,

$$
\begin{aligned}
u &= 2.640 + 1.05\ w && , T_a - T_w \le -10.5 \\
&= 2.350 + 1.01\ W && , -10.5 < T_a - T_w \le -3.5 \\
&= 1.141 + 0.92\ W - 0.28\ (T_a - T_w) && , -3.5 < T_a - T_w \le 3.5 \\
&= 2.687 + 0.49\ W - 0.02\ T_a && , 3.5 < T_a - T_w \le 10.5 \\
&= 3.317 + 0.32\ W - 0.02\ T_a && , T_a - T_w > 10.5
\end{aligned}
\qquad (15)
$$

$$
\begin{aligned}
T &= -2.034 + 0.60\ T_a + 0.54\ T_w && , T_a - T_w \le -10.5 \\
&= -0.696 + 0.67\ T_a + 0.42\ T_w && , -10.5 < T_a - T_w \le -3.5 \\
&= 0.290 + 0.47\ T_a + 0.52\ T_w && , -3.5 < T_a - T_w \le 3.5 \\
&= 2.110 + 0.29\ T_a + 0.65\ T_w && , 3.5 < T_a - T_w \le 10.5 \\
&= 2.945 + 0.30\ T_a + 0.56\ T_w && , T_a - T_w > 10.5
\end{aligned}
\qquad (16)
$$

$$
\begin{aligned}
D &= -5.115 + 0.56\ D_l + 0.46\ T_w && , T_a - T_w \le -10.5 \\
&= 0.240 + 0.94\ D_l + 0.11\ T_w && , -10.5 < T_a - T_w \le -3.5 \\
&= -0.350 + 0.72\ D_l + 0.31\ T_w && , -3.5 < T_a - T_w \le 3.5 \\
&= -0.160 + 0.44\ D_l + 0.55\ T_w && , 3.5 < T_a - T_w \le 10.5 \\
&= 0.790 + 0.43\ D_l + 0.53\ T_w && , T_a - T_w > 10.5
\end{aligned}
\qquad (17)
$$

2.3 Ice Cover

Because the lakes experience significant ice cover during the winter season, the estimated evaporation must be corrected for the effects of ice. This is done here by using temperatures and specific humidities over ice for the over-ice evaporation calculation in (10) and over water for the over-water calculations; the two estimates are then combined by weighting for the fraction of the surface covered with ice. Existing data on ice cover (Assel, 1983a) were used to determine empirical relations between ice cover extent and air temperatures, in a manner similar to other efforts (Derecki, 1978, 1981a):

$$I = MAX(\ MIN(\ c_1 - c_2\ \Upsilon_a - c_3\ \Upsilon_{a-1}, 1.0),\ 0.0) \qquad (18)$$

where I = monthly average fraction of the surface covered by ice, cl, c_2, and c_3 are empirical coefficients for a given lake and month, Υ_a = monthly average over-land air temperature (°C), and Υ_{a-1} = monthly average over-land air temperature (°C) for the preceding month. The empirical coefficients for (18) are given in Table 2.

Table 2.--Ice cover coefficients, c_i

Month	c_1	c_2 $(°C)^{-1}$	c_3 $(°C)^{-1}$	c_1	c_2 $(°C)^{-1}$	c_3 $(°C)^{-1}$
	Superior			Michigan		
Jan	-0.314387	-0.012352	-0.027498	-0.108262	-0.016680	-0.012855
Feb	-0.455670	-0.008526	-0.045248	-0.116667	-0.017650	-0.018551
Mar	-0.404057	0.006066	-0.072318	-0.011612	0.001294	-0.010892
Apr	0.201811	-0.028747	-0.000638	-0.000429	0.004148	-0.011771
Dec	-0.028608	-0.004238	0.000910	0.001165	-0.004570	-0.007143
	Huron			St. Clair		
Jan	-0.035293	-0.015755	-0.016502	0.4091	-0.05918	-0.01517
Feb	-0.18775	-0.031164	-0.048973	0.6303	-0.0420	-0.02145
Mar	-0.13003	-0.032276	-0.060014	0.3829	-0.1042	-0.06507
Apr	0.230864	-0.021162	-0.06788	0.5122	-0.0717	-0.04211
Dec	0.0	0.0	0.0	0.2329	-0.08165	-0.04300
	Erie			Ontario		
Jan	0.0400	-0.05361	-0.05867	-0.0586	-0.018725	0.000276
Feb	0.5286	-0.03375	-0.01885	-0.14067	-0.0313	-0.016876
Mar	0.2272	-0.04713	-0.06002	-0.081346	0.004778	-0.03738
Apr	0.1133	-0.00266	-0.018	-0.000144	0.007138	0.012394
Dec	0.0896	-0.0234	-0.01518	0.0	0.0	0.0

2.4 Daily Calculations

For each day, given W, T_a, D_l, and T_w, calculate U, T, and D from (12), (13), and (14) or from (15), (16), and (17), determine the specific humidity of the air, q, from D with standard psychrometric relations for water vapor pressure, and determine the specific humidity at the surface, q_w, from T_w at saturation. Compute the bulk evaporation coefficient CE from U, T, and T_w with (1), (4), (5), (7), (9), and (11), and find the over-water evaporation E_w from (10). For over-ice conditions, use W, T_a, D_l, and T_w = MIN (T_a, 0) (for temperatures measured in degrees Celsius) to calculate U, T, and D from (12), (13), and (14) or from (15), (16), and (17) representing over-ice meteorology, determine the specific humidity q from D with standard psychrometric relations, and determine the specific humidity at the ice surface q_w from T_w = MIN (T_a, 0) at saturation with psychrometric relations for vapor pressure over an ice surface. Compute the bulk evaporation coefficient CE from U, T, and T_w = MIN (T_a, 0) with (1), (4), (5), (7), (9), and (11), and find the over-ice evaporation Ei ($= E_w$) from (10). Finally, find ice cover from (18) and compute total evaporation from

$$E = (1 - I)\, Ew + I\, Ei\,. \qquad (19)$$

Note that ice temperature should be T_w = MIN (T, 0) for temperatures measured in degrees Celsius but T is a function of T_w. In light of the approximations of using over-water correction equations for over-ice corrections and of using relations for CE derived over water for over-ice conditions, it is not deemed worthwhile to find T and T_w simultaneously for ice. In fact, in agreement with Schertzer (1978),

ice (as it affects evaporation) could just as easily be ignored with the current understanding of, and data availability for, over-ice evaporation. The approach just described is probably no more accurate than this simple assumption; however, the approach is taken so that, if or when better over-ice data become available in the future, they may be used in this approach.

3. HEAT STORAGE

3.1 Temperature Profile

In their comparison of seasonal thermocline models with observations, Gill and Turner (1976) found that the most satisfactory comparison between North Atlantic sea surface temperatures and simple point models was a version of the model of Kraus and Turner (1967), in which a mixed layer is produced by both mechanical and (in the cooling period) convective mixing. In the heating season, the process carries heat downward from the atmospheric input at the surface by mixing, dissipation, and internal wave energy. As Gill and Turner (1976) explained Kraus and Turner's model, "when the heating rate is increasing [at the surface], a surface mixed layer is found above a smooth profile, and there are no temperature discontinuities. The mixed layer depth decreases with time, but the smooth profile below does not alter once it is established. When the heating rate stops increasing, the temperature discontinuity develops at the base of the mixed layer, and the mixed layer depth starts to increase. The temperature at a given depth below the mixed layer is constant until that point is engulfed by the mixed layer."

This general behavior is widely recognized to occur in large lakes and is seen from inspection of Fig. 2, where averaged bathythermograph data from Lake Superior for 1972-79 (Assel, 1983b, 1985) are plotted. Spring turnover occurs around June for Superior (when temperatures are everywhere 3.98°C, the temperature for maximum density of water). As surface temperature begins increasing above 3.98°C, a stable profile develops; surface temperature increases faster than temperatures at depth, until a well-defined layer is present at the end of the summer. because the net heat flux to the surface then changes to negative, surface temperature drops and the temperatures at depth first grow and then recede, keeping the upper part of the profile vertical. The mixed layer (where the temperature profile is vertical) deepens until the profile again approaches a vertical line throughout at 3.98°C (representing fall turnover late in the year for Superior). This approach to fall turnover is well illustrated in Fig. 2 by the temperature profiles during the latter part of the year for 1976, 1977, 1978, and 1979. Then a symmetrical behavior is observed with temperatures less than 3.98°C as the lake continues to lose heat; the surface temperature changes faster until the net heat flux at the surface changes to positive again (see 1973 in Fig. 2). Surface temperature then increases toward 3.98°C and the temperatures at depth first decrease and then increase as the profile again approaches a vertical line (representing spring turnover); this progression is best illustrated by the profiles for early 1976 in Fig. 2.

3.2 Stored Heat

There is a hysteresis in the heating and cooling cycles of the lakes (reflected in Fig. 2) since the relationships between heat in the lake and surface temperature differ from each other during these cycles. As surface temperature climbs through the spring turnover, heat in the lake is increasing relatively quickly with surface temperature but the rate soon decreases since mainly surface waters are affected; as surface temperature approaches its peak, heat in the lake begins increasing more quickly with surface temperature again, as heat migrates down from the surface. After the surface temperature has peaked and begins to drop, the heat in the lake continuously slows its ascent until it peaks slightly later than did the surface temperature. As the lake then begins cooling, heat changes (drops) more and more quickly with (dropping) surface temperature since successively deeper layers are involved in the convective mixing, and the lake approaches fall turnover (heat approaches capacity at turnover). Likewise, as

surface temperature approaches its minimum, the heat deficiency (heat capacity at turnover minus the heat stored) per degree of surface temperature drops and rises, and then it drops after minimum surface temperature is reached; it then increases again as surface temperature rises toward the spring turnover.

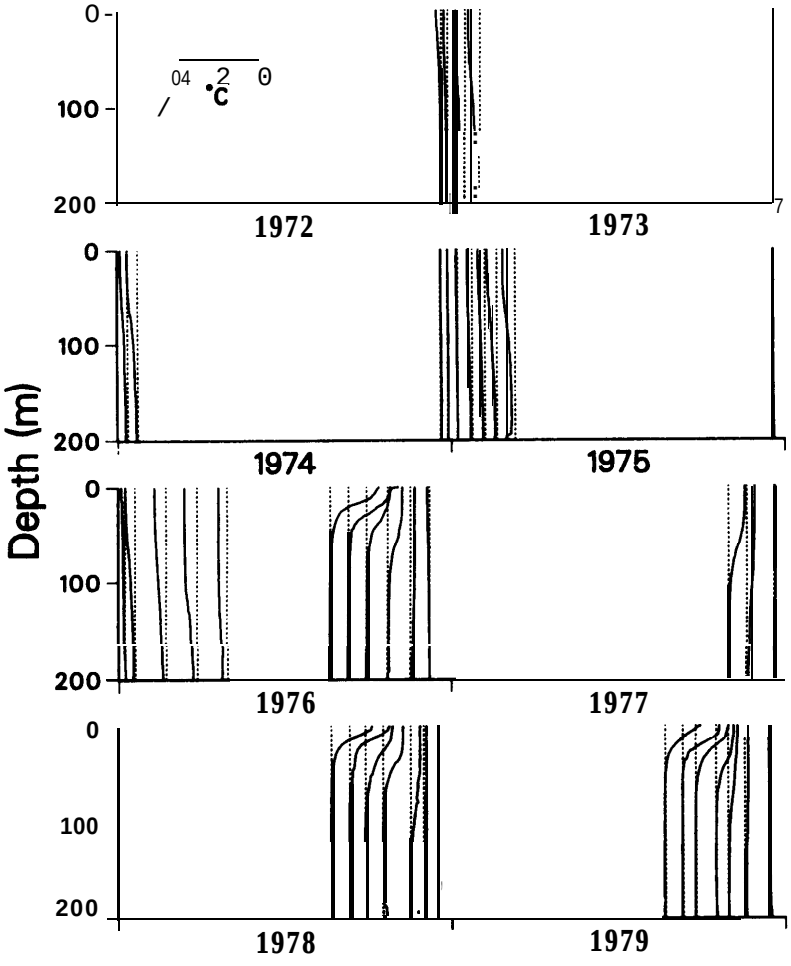

Figure 2.-Area1 average profiles of Lake Superior temperature.

After the spring turnover then (or anytime surface temperature is above 3.98°C), if heat is added uniformly throughout a surface layer of depth y, we can write the heat addition increases with (surface) temperature as (for daily additions)

$$H_j - H_{j-1} = r_w\, C\, A(-y/2)\,(T_j - T_{j-1})\, y \qquad , H_j \geq H_{j-1} \geq H_d \qquad (20)$$

where H_j = heat in storage in the lake at the end of day j (j days after the last spring turnover), C = specific heat of water, A(Z) = area of the horizontal plane at height Z above the water surface, Tj = surface temperature (T_w) at the end of day j, and Hd = heat in storage at turnover (when the surface temperature, as well as temperatures at all depths, is 3.98°C). More generally, heat additions penetrate non-uniformly to various depths, and for the prismatic case [in which the lake is treated as a cylinder over the penetration depth, A(Z) = A, $0 \leq Z \leq -y$],

$$H_j = H_{j-1} + a\,(T_j - T_{j-1})^c \qquad , T_j \geq T_{j-1} \geq T_d \qquad (21)$$

where a and c are empirically derived parameters and Td = temperature of maximum water density (3.98°C). Old heat additions continue penetration (through processes of conduction, diffusion, and mechanical mixing while temperatures are increasing); their effect on surface temperature rise diminishes and an aging function can reflect this:

$$H_m = H_{m-1} + a\,[1 + b\,(j - m)^x]\,(T_m - T_{m-1})^c \qquad , 0 < m \leq j$$

$$H_0 = H_d \tag{22}$$

$$T_0 = T_d$$

where b and x are empirically derived parameters. Temperature increments from past heat additions are "added" by superimposing the effects of past daily heat additions to determine the surface temperature. An alternate expression of this superposition can be made in terms of the surface temperature. For the case of continuous heat additions every day, repeated application of (22) gives

$$T_j = T_0 + \sum_{m=1}^{j} \{\tfrac{1}{a}\,(H_m - H_{m-1}) / [1 + b\,(j - m)^x]\}^{1/c} \tag{23}$$

If heat is removed, it comes from the surface layers, lowering surface and near-surface temperatures, which results in convective mixing and a deepening of the mixed layer. The most recent heat additions are arbitrarily removed first since they are most available for release (they are less distributed with depth than older additions and have their major fraction closest to the surface). If $Hj < H_{j-1}$, then

$$Hj = Hk + a\,[1 + b\,(j - k - 1)^x]\,(Tj - T_k)^c \qquad , T_j \geq T_k \geq T_d \tag{24}$$

where k is determined such that

$$H_{k+1} > H_j \geq H_k \geq H_d\,. \tag{25}$$

Surface temperature varies with heat in storage, as given by (23), until a recent heat addition is used up; then the next earlier heat addition is depleted. Equivalently, Hj also can be given by (22) by replacing H_m with Hj for $m > k$; that is, all H_m greater than Hj are replaced with Hj in (22), which is equivalent to eliminating the mth equation in (22).

More generally, heat is added, then removed, then added, and so forth, and although recent additions may be lost, new additions will occur. For the general case, in which heat additions and losses may follow one another, (23) becomes

$$T_j = T_0 + \sum_{m=1}^{j} \{\tfrac{1}{a}\,(\underset{m \leq n \leq j}{\text{MIN}}\, H_n - \underset{m-1 \leq n \leq j}{\text{MIN}}\, H_n) / [1 + b\,(j - m)^x]\}^{1/c} \tag{26}$$

where

$$\underset{m \leq n \leq j}{\text{MIN}}\, H_n = \text{MIN}(H_m, H_{m+1}, \ldots, H_{j-1}, H_j)\,. \tag{27}$$

A symmetrical expression for heat losses, similar to (26), can be derived for surface temperatures below Td (after fall turnover) but experience shows that the use of the same equation for all variations of heat and temperature (no superposition) is adequate:

$$Hj = Hd - a' [1 + b' j^{x'}] (Td - T_j)^{c'} \quad (28)$$

where a', b', c', and x' are empirically derived parameters and j is measured from the day of the fall turnover.

In the use of (26) and (28), as well as in the estimation of their parameters (calibration), a limit is placed on the effect of aging; after j-m > 182 days (arbitrarily chosen), the aging function $1 + b (j-m)^x$ is taken as constant. Also, in computing implementations of (26), only 182 terms or less need be computed for the summation; since early terms older than 182 days (with a constant aging function value) can be combined into a single term with some equivalent "replacement" age, then the first two terms of the summation in (26) can be replaced with the single term that uses the end-of-day heat storage of the second term $(H_2), H_0$, and the replacement age. In general, the replacement age for the next day's oldest heat addition can be found from the present replacement age so that the oldest terms can be combined. Finally, note that any term in the summation in (26) that becomes zero,

$$\underset{m \le n \le j}{\text{MIN}}\, H_n - \underset{m-1 \le n \le j}{\text{MIN}}\, H_n = 0,$$

will always be zero on subsequent days; it can be eliminated from all further consideration whenever heat in storage drops below a past value.

Several aging functions and other variations of (22) were investigated including linear and exponential temperature difference terms, aging functions, and their combinations. Better proxies might be constructed for the aging function, especially since wind speed is available in the data set. However, (26) and (28) preserve essential features. Turnovers can occur as a fundamental behavior of (26) and (28). Hysteresis between H and T_w is present because the aging function increases with time. This implies that more heat is stored or lost per degree change in surface temperature with age. A related effect is given by the temperature difference term power (c or c'). For c (or c') smaller than unity, there is a bigger change in heat storage (or heat deficiency) per degree of surface temperature for lower surface temperatures than for higher ones (for c greater than unity this is reversed). These two effects both give rise to types of hysteresis and are offsetting but related to different aspects of the process (time and temperature). Furthermore, each dominates at different parts of the process. The trade off between these two effects is controlled of course by the values of the coefficients: a, b, c, x, a', b', c', and x'.

4. HEAT BUDGET

4.1 Fluxes Over Water

Heat in storage in the lake at the end of each day is given by a simple conservation of energy (energy used in ice formation and decay is accounted for separately):

$$H_{j+1} = H_j + [(1 - I) A (Q_i - Q_r + Q_l - Q_e + Q_P) + Q_I - Q_O] d + Q_m + o \quad (29)$$

where A = area of the lake surface, j = the number of the day for which the following fluxes apply, Q_i = average daily rate of incident short-wave radiation to a unit area, Q_r = average daily rate of short-wave radiation reflected from a unit area of surface, Ql = average daily rate of net long-wave radiation exchanged between the atmosphere and a unit area of surface, Q_e = average daily rate of evaporative and sensible heat transfers from a unit area, Q_P = average daily energy advection rate into the lake by precipitation on a unit area of surface, QI = average daily energy advection rate into the lake by runoff and river inflow, Q_O = average daily energy advection rate out of the lake, d = time in one day, Q_m = correction to heat balance for the disappearance of the ice cover during the day (since some of the energy flux computed over ice applies over water) and o = other terms (including heat transfer through the

bottom of the lake) that are neglected here. The average daily incident short-wave radiation rate is taken here as (Gray et al., 1973)

$$Q_i = [0.355 + 0.68\,(1 - N)]\,Q_o \tag{30}$$

where N = cloud cover expressed as a decimal fraction, and Q_o = average daily short-wave radiation rate received on a horizontal unit area of the Earth's surface under cloudless skies, interpolated for date from generalized maps of mid-monthly values, as reported by Gray et al. (1973) for Canadian and northern U.S. positions, that include effects of water content of the atmosphere, air mass, and other factors (Table 3). More physically-based models for solar radiation might be used but would require more extensive data than available here and might not then be usable in forecast or simulation settings. The average daily reflected short-wave radiation rate Q_r is taken here simply as one-tenth of the incident, after Gray et al. (1973), as an average for a water surface. Alternatively, monthly mean albedo over water could be used as derived during IFYGL (Davies and Schertzer, 1974).

The daily net long-wave radiation exchange between the atmosphere and a water surface, Ql, is derived from considerations of radiation from a water body and the atmosphere as affected by cloud cover. Considering a water body as a gray body, long-wave radiation from the surface (Gray et al., 1973) is

$$Q_u = 0.97\ 5.67 \cdot 10^{-8} (T_w + 273.16)^4 \tag{31}$$

where Q_u = average daily long-wave radiation rate from a unit area of water surface ($W\,m^{-2}$), 0.97 = the emissivity of water, $5.67 \cdot 10^{-8}$ = the Stefan-Boltzmann constant ($W\,m^{-2}\,K^{-1}$), and 273.16 = the freezing temperature in kelvins. The counter-radiation from a clear sky is estimated (Keijman, 1974) as

$$Q_d = 5.67 \cdot 10^{-8}\, T_a'^4\, (0.53 + 0.065\, e_a^{1/2}) \tag{32}$$

where Q_d = average daily long-wave radiation rate from the atmosphere ($W\,m^{-2}$), T_a' is the air temperature (K), and e_a is the vapor pressure of the air (mb) at the 2-m height. The expression in parentheses in (32) is for atmospheric emissivity after Keijman (1974), Kramer (1957), and U.S. Geological Survey (1954). Most often (31) and (32) are added algebraically as the net exchange and then a correction is made to this total for cloudiness (Gray et al., 1973; Penman, 1948). However, cloud cover affects atmospheric radiation and not the surface radiation; the correction is made only to (32) and the two equations are combined [Keijman (1974)] to give net long-wave radiation rate per unit of surface in ($W\,m^{-2}$)

$$Q_l = 5.67 \cdot 10^{-8}\, T_a'^4\, (0.53 + 0.065\, e_a^{1/2})\, [p + (1 - p)\,(1 - N)] - 0.97\ 5.67 \cdot 10^{-8} (T_w + 273.16)^4 \tag{33}$$

Table 3.--Average mid-month cloudless daily insolation ($W\,m^{-2}$)[a]

Lake	Jan	Feb	Mar	Apr	May	Jun	Jul	Aug	Sep	Oct	Nov	Dec
Superior	92	160	238	310	373	383	373	325	247	175	97	73
Huron	92	160	238	310	373	383	373	325	247	175	97	73
Michigan	107	165	233	301	339	354	339	296	238	175	116	92
St. Clair	107	162	228	296	344	366	351	308	250	184	121	92
Erie	107	162	228	296	344	366	351	308	250	184	121	92
Ontario	97	155	223	288	337	359	342	298	240	175	111	87

[a] 1 $W\,m^{-2}$ = 2.063 cal $cm^{-2}\,day^{-1}$

where p is an empirical coefficient that reflects the effect of cloudiness on the atmospheric long-wave radiation to the Earth.

The average daily rate of evaporative and sensible heat transfers, Q_e, consists of latent heat of evaporation, advected heat of evaporation, and sensible heat transfer; the last of these is taken as the latent heat of evaporation times Bowen's ratio (Gray et al., 1973).

$$Q_e = r_w [(1 + B) v + C T_w] E_w \tag{34}$$

where v = the latent heat of vaporization and B = the Bowen ratio, given (Gray et al., 1973) as

$$\begin{aligned} B &= 0.00061 \text{ Pa } (T_w - \text{Ta}) / (e_w - e_a) && , e_w - e_a \geq 0.001 \\ &= 0 && , e_w - e_a < 0.001 \end{aligned} \tag{35}$$

where e_w = saturation water vapor pressure at T_w (mb) and Pa = atmospheric pressure (mb).

Energy advected with precipitation occurs at the rate

$$\begin{aligned} Q_P &= r_w (C T_a - f) P && , T_a < 0 \\ &= r_w C T_a P && , T_a \geq 0 \end{aligned} \tag{36}$$

where f = the heat of fusion for water, P = precipitation rate expressed as a depth per unit time, and T_a is in degrees Celsius. When the air temperature is below freezing, precipitation is treated like snow and the heat of fusion is removed from the surface as the snow melts. Advection of the energies into and out of the lake with other water flows occurs at the rates, respectively, of

$$Q_I = R r_w C T_w \tag{37}$$

and

$$Q_O = O r_w C T_w \tag{38}$$

where R = runoff (from the basin to the lake) and river flow rates to the lake and 0 = river flow rate from the lake, and T_w is in degrees Celsius.

4.2 Fluxes Over Ice

The heat delivered to the ice cover each day, H', is given by a simple account of energy fluxes:

$$H' = I A (Q_i - Q_r' + Q_l' - Q_e' + Q_P') d + o' \tag{39}$$

where Q_r' = average daily rate of short-wave radiation reflected from a unit area, Ql' = average daily rate of net long-wave radiation exchanged between the atmosphere and a unit area, Q_e' = average daily rate of evaporative and sensible heat transfers from a unit area of ice surface, Q_P' = average daily energy advection rate onto a unit area by precipitation on the ice surface, and o' = other terms ignored here as neglibile. The average daily reflected short-wave radiation rate, Q_r', is taken here (Gray et al., 1973) as

$$Q_r' = (0.85 \text{ In} + 0.70 \text{ Io} + 0.50 \text{ Im} + 0.45 \text{ Ib}) Q_i \tag{40}$$

where I, = fraction of the ice covered with new snow, I, = fraction of the ice covered with old snow, I,,, = fraction of the ice covered with melting snow, and Ib = fraction of the ice that is bare of snow. Because data are unavailable for these fractions and because the heat budget is not sensitive to this small heat loss, the first three fractions are taken as zero and the fourth as unity. Differences with actual conditions can give rise to large differences in the albedo represented by (40).

The daily net long-wave radiation exchange between the atmosphere and an ice surface, Q_l', is found from (33); this is equivalent to ignoring the ice cover for net long-wave exchange with the atmosphere; ice cover probably does have some effect on the exchange, but the variation between thermal radiation from open water and from ice-covered water is ignored. The average daily rate of evaporative and sensible heat transfers from ice, Q_e', consists of latent heat of evaporation, heat of fusion, advected heat of evaporation at the temperature of the ice surface [MIN (T_a, 0) for temperatures in degrees Celsius], and sensible heat transfer. The last of these is difficult to estimate accurately but is taken here as the latent heat of evaporation times Bowen's ratio calculated by using ice surface temperature.

$$Q_e = r_w [(1 + B') v' + f + C \, MIN(T_a, 0)] E_i \qquad (41)$$

where v' = the latent heat of vaporization evaluated at the temperature of the ice [MIN (T_a, 0)], and B' = the Bowen ratio evaluated from (35) with T_w = MIN (T_a, 0). Finally, energy advected with precipitation onto the ice surface occurs at the rate

$$Q_P' = r_w C T_a P \qquad (42)$$

The heat delivered to the ice cover each day, H', can be used in a heat balance over the ice to adjust the ice cover mass for accumulation, aggradation, and ablation:

$$\begin{aligned} M_2 &= M_1 - H' / f / r_i && , H' / f / r_i \le M_1 \text{ and } I > 0 \\ &= o && , H' / f / r_i > M_1 \text{ or } I = 0 \end{aligned} \qquad (43)$$

where Ml and M2 are the masses of the ice cover at the beginning and end of the day respectively, and the heat correction to (29) for the disappearance of the ice cover during the day is

$$Q_m = H' - (M_1 - M_2) f r_i . \qquad (44)$$

The use of MIN (T_a, 0) as ice surface temperature is an approximation that could conceivably be improved by keeping track of an ice temperature in the heat balance for the ice cover, but with the uncertainties in the ice heat flux terms and especially in the evaluation of over-ice albedoes, such a calculation is inappropriate.

4.3 Heat Balance

Because both surface temperature and evaporation over water and ice are unknown and must be determined each day, an iterative approach is used. The surface temperature at the beginning of the day is determined inversely with (26) or (28) from the heat storage at the beginning of the day (which is equal to the heat storage at the end of the previous day). The surface temperature at the end of the day is initially set equal to that at the beginning. Then 1) the beginning and end surface temperatures are averaged as the surface temperature during the day; 2) the average is used with the day's meteorology to compute evaporation over water and ice from (1), (4-5), (7), and (9-19); 3) stored heat at the end of the day is found from the balances of (29) and (39) with fluxes determined by (30), (33-38), and (40-44); and 4) an improved surface temperature at the end of the day is computed by solving (26) or (28) again. These four steps are repeated until the surface temperature at the end of the day converges to within 0.001°C. If the surface temperature reverses or passes through 3.98°C (turnover), the appropriate equation is utilized [(26) or (28)].

Computation of end-ofday surface temperature in step 4 is constrained to above-freezing temperatures even though the heat in the lake is allowed to drop below the amount corresponding to freezing surface temperatures on a given day. This represents a departure from the assumed heat storage of (28), possibly the result of additional ice formation not accounted for separately in the model. The

energy is balanced in the model with surface temperatures held at freezing until sufficient heat is again in storage to allow surface temperatures to rise, possibly the result of additional ice melt not accounted for separately in the model.

5. APPLICATION

5.1 Calibration

Remotely-sensed surface temperatures from 1) the National Oceanic and Atmospheric Administration's series of Polar Orbiting Satellites Advanced Very High Resolution Radiometer (for 1980-present [Irbe and Saulesleja, 1982; Irbe et al., 1982; Atmospheric Environment Service, 1988]) and 2) the Atmospheric Environment Service's (AES) airborne surveys of water surface temperatures (for 1966-1980 [Irbe, 1972]) were reduced for all Great Lakes except Michigan by the Hydrometeorology Division of AES. The Canadian Climate Centre currently uses the 10.5-micron infrared channel from both daily passes of both satellites and calculates atmospheric corrections from radiosonde data; they report a 0.5°C root-mean-square error between the satellite-derived temperatures and available buoy temperatures. The reported temperatures are instantaneous values obtained through interpretation of both visible (for cloud and ice cover) and infrared pictures of the Great Lakes and may be higher than is representative for a daily average. Since there is a larger diurnal range of surface temperatures during higher temperatures, direct use of these instantaneous values gives evaporation estimates unrepresentative of average daily losses. Other problems include an imprecise knowledge of satellite locations, a fair-weather bias (since daytime observations are used with clear or mostly clear skies, light winds, and an absence of steam fog on the lakes), and an avoidance of the split-channel technique of extracting surface temperatures (an empirical approach used widely for producing sea surface temperatures globally) since it does not work well over land and lakes. However, these measurements form an independent set of data that may be used for comparisons in evaporation calculations.

The heat balance model is calibrated to determine values of the seven (7) parameters (a, b, c, a', b', c', and p) with x = x' = 1 that give the smallest sum-of-squared-errors between model and actual daily surface temperatures observed by satellite during a calibration period. The surface temperature and the ages and amounts of past heat additions must be initialized prior to modeling or calibration. If the model is to be used in forecasting or for short simulations, then it is important to determine these variables accurately prior to use of the model. If the model is to be used for calibration or for long simulations, then the initial values are generally unimportant. The effect of the initial values diminishes with the length of the simulation and after l-2 years of simulation, the effects are nil from a practical point of view. Calibrations were performed over the last few data-rich years, 1978-85, and were verified by comparison with the earlier years, 1965-77. No data were used in the calibrations until 1980 to allow sufficient initialization. Since the period began 1 January 1979, $T_W = 0$ and j = 0 were arbitrarily used.

Parameters are determined in an automated systematic search of the parameter space to minimize the sum-of-squared-errors between actual and model surface temperatures, similar to methods described elsewhere for calibrating rainfall-runoff models (Croley and Hartmann, 1984). Each parameter, selected in rotation, is searched until all parameter values converge to three digits instead of searching until the sum-of-squared-errors stabilizes. Such an approach is important where synergistic parameter, interactions allow the parameters to change even after the sum-of-squared-errors has stabilized. The heat balance model with (26), (28), and x = x' = 1 was found to best match observed temperatures of all functions tried; marginal improvements were then observed by setting x = 4 and x' = 1. Calibration results are summarized in Table 4. Note in Table 4 that many parameters appear to be specified sufficiently by two digits (the third digit is zero). This is an artifact of the calibration process. The search of the parameter space is managed first by changes in single-digit parameter values, for each of the parameters, until the minimum sum-of-squared-error is found; then changes in the second digit are allowed until the minimum is found, and then changes in the third digit are allowed until the minimum

Table 4.--Daily calibration results

		Lake				
		Superior	Huron	St. Clair	Erie	Ontario
Surface Area, km^2		82100	59600	1114	25700	18960
Volume, km^3		12100	3540	3.3	484	1640
Average Depth, m		147	59.4	3.05	18.8	86.5
CALIBRATED PARAMETER VALUES						
a,	10^{20} cal deg^{-c}	$.200 \cdot 10^{-1}$	.105.10-1	$.975 \cdot 10^{-4}$	$.421 \cdot 10^{-2}$	$.308 \cdot 10^{-2}$
b,	day4	$.381 \cdot 10^{-7}$	$.118 \cdot 10^{-7}$	0	0	$.110 \cdot 10^{-7}$
c		$.981 \cdot 10^{+0}$	$.836 \cdot 10^{+0}$	$.930 \cdot 10^{+0}$	$.104 \cdot 10^{+1}$	$.899 \cdot 10^{+0}$
a′,	10^{20} cal $deg^{-c'}$	$.376 \cdot 10^{-1}$	$.309 \cdot 10^{-1}$	$.716 \cdot 10^{-3}$	$.984 \cdot 10^{-2}$	$.431 \cdot 10^{-2}$
b′,	day^{-1}	$.200 \cdot 10^{-1}$	$.100 \cdot 10^{-9}$	$.100 \cdot 10^{-9}$	$.100 \cdot 10^{-9}$	$.312 \cdot 10^{-1}$
c′		$.981 \cdot 10^{+0}$	$.987 \cdot 10^{+0}$	$.299 \cdot 10^{+1}$	$.823 \cdot 10^{+0}$	$.801 \cdot 10^{+0}$
p		$.149 \cdot 10^{+1}$	$.133 \cdot 10^{+1}$	$.128 \cdot 10^{+1}$	$.157 \cdot 10^{+1}$	$.133 \cdot 10^{+1}$
CALIBRATION PERIOD STATISTICS (1979-85)[a]						
Number of Observations		110	165	64	150	189
Means Ratio[b]		1.05	0.99	1.09	1.03	0.98
Variances Ratio[c]		0.95	0.97	1.34	1.16	0.98
Correlation[d]		0.98	0.98	0.97	0.98	0.98
R. M. S. E.[e]		1.20	1.32	2.81	1.95	1.48
VERIFICATION PERIOD STATISTICS (1966-78)						
Number of Observations		94	160		104	149
Means Ratio[b]		0.95	0.98		1.12	1.05
Variances Ratio[c]		1.11	0.99		1.42	1.02
Correlation[d]		0.93	0.98		0.97	0.98
R. M. S. E.[e]		1.62	1.26		2.76	1.57
COMBINED PERIOD STATISTICS (1966-85)						
Number of Observations		204	325	64	254	338
Means Ratio[b]		1.00	0.99	1.09	1.07	1.01
Variances Ratio[c]		1.00	0.97	1.34	1.25	0.99
Correlation[d]		0.96	0.98	0.97	0.97	0.98
R. M. S. E.[e]		1.41	1.29	2.81	2.31	1.52

[a]Data between 1 January 1979 and 31 December 1985 for all Great Lakes and between 1 January 1979 and 31 December 1983 for Lake St. Clair.
[b]Ratio of mean model surface temperature to data mean.
[c]Ratio of variance of model surface temperature to data variance.
[d]Correlation between model and data surface temperatures.
[e]Root-mean-square error between model and data surface temperatures in degrees Celsius.

is found. Since some parameters do not change beyond the first or second digit, we observe that parameter compensation is taking place, indicating that the model is over-specified in terms of the number of parameters. Some of the parameters probably could be combined in a reformulation of the heat storage equations.

The goodness-of-fit statistics for the-calibration and verification periods in Table 4 show generally good fits on the deep lakes between the actual and calibrated-model surface temperatures; correlations are high and means and variances are close between the data and model for each lake. The root-mean-square error is about 1.2°C for Lake Superior (1.6" over the verification period), 1.3" (1.3") for Lake Huron, 2.8° for Lake St. Clair, 2.0" (2.8°) for Lake Erie, and 1.5" (1.6") for Lake Ontario. The worst error on the deep lakes is only 1.6° for Lakes Superior and Ontario during the verification periods. It was necessary to set parameter b to zero for the St. Clair and Erie calibrations; the minimum allowed by the calibration procedure, $0.1 \cdot 10^{-9}$, was still too big to be feasible on these shallow lakes. Note that the calibrated value of the exponent, c in (26), is the closest to unity for Lake Erie of all of the calibrations. This is consistent with shallow-lake concepts in which the water throughout the depth is at the same temperature (and equal to the surface temperature) between spring and fall turnovers. The heat in the lake is described best then by a linear function of surface temperature.

Note that the goodness-of-fit for each lake, in terms of the root-mean-square error during the calibration period, varies inversely with the volume of the lake. This suggests that the heat storage superposition model is most applicable to the deep lakes and presumably fails on the shallower lakes where mechanical mixing of the shallow lakes by winds is poorly represented by the aging function. However, other calibrations, not shown here, in which the black body long-wave radiating temperature was taken as a linear function of the heat in storage (two additional parameters) and in which the lake evaporation coefficient was allowed to float (one additional parameter), gave a root-mean-square error on Erie of 1.2°C instead of 2.0" (there were only small differences on the deep lakes). Unfortunately, there is little physical basis for those modifications and additional parameters; it is not possible to explain the improved goodness-of-fit or to have much confidence in applying the resulting model to meteorologic conditions outside of those represented in the data set (such as various climate change scenarios). Nevertheless, while the extra degrees-of-freedom allowed better matching of water surface temperatures, wind data were not utilized any more than in the present model. Conceptual model improvements may then be possible not only by considering wind data in improved mixing models for shallow lakes but also by considering changes in heat fluxes more appropriate for shallow lakes.

Of course, there are many sources for error including the model concepts for heat storage, heat balance, evaporation, ice cover, and over-water corrections, the satellite observations themselves, and the over-land meteorological data at stations about each lake. The good agreement between model and observations is no doubt partially due to somewhat compensating errors.

Figure 3 contains surface temperatures calculated with the Lake Ontario application of the model calibration summarized in Table 4, as applied to historical meteorological data over the calibration and verification periods. It is very typical of the behavior and agreement found on Lakes Superior, Huron, St. Clair, and Erie even though it is the poorest fit among the deep Great Lakes. Temperature plots for the other lakes are contained in Appendix A. Lake Ontario was chosen for display since Lake Ontario has the most satellite observations (see Table 4). Figure 3 shows that turnover is predicted within about 1 to 2 weeks most of the time; above-freezing winters are replicated (as much as can be seen from the scanty data) most of the time; late-summer peaks in surface temperature appear poorly duplicated (when there are data at those times) and the model consistently underestimates them. However, this latter observation is consistent with the recognized fair-weather and day-time bias to the data. The larger diurnal range of surface temperatures during periods of high temperatures means that instantaneous values can be unrepresentative of daily averages and may be higher (Irbe, personal communication).

Inspection of the Lake St. Clair surface temperatures in Appendix A reveals behavior of the model not observed on any of the other lakes. Winter temperatures from the model never drop below about

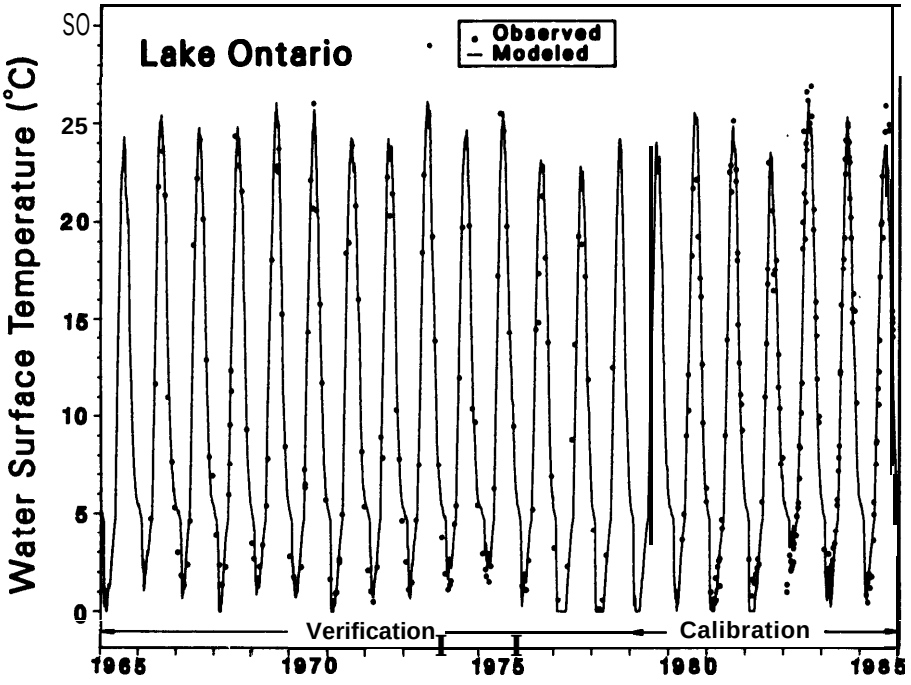

Figure 3.--Lake Ontario water surface temperature.

3.3°C which is clearly in error. This probably results from calibration with a limited data set that contains only a few winter temperature data points. A second problem may be in the application of the model to such a small shallow lake with almost no heat storage capability.

5.2 Evaporation and Heat Fluxes

The estimation of water surface temperatures makes it possible to calculate all components of the heat balance including evaporation. Figure 4 shows the average daily over-water meteorology, surface temperature, and evaporation for Lake Ontario; they were prepared by applying the model calibration for Lake Ontario in Table 4 to data over the period 1948-1985 and averaging the 36 annual cycles for 1950-1985. This display allows inspection of general behavior while filtering high-frequency fluctuations. Similar plots for other lakes are contained in Appendix B. Since the lake is moderating the overlying meteorology, air temperatures and surface temperatures appear to peak at about the same time although the surface reaches its minimum temperature a month after the atmosphere. However, surface and over-water air temperatures peak about 2 weeks after over-land air temperatures (not shown). This shift is even more pronounced on the northern Great Lakes; Superior and Huron have shifts of about a month. Fluctuations in monthly evaporation are tied most strongly to fluctuations in humidity and wind speed. Monthly evaporation is strongest in the fall and winter; wind speed peaks in the winter; air temperature and net radiation (incident short wave and long wave) peak in midsummer to late summer. Evaporation peaks on all lakes in September and again on the deep lakes in December or January. The first peak results from the high surface temperatures and dropping humidities that occur in the fall. On the deeper lakes, this effect lasts into the winter as surface temperatures drop more slowly. The second peak occurs on the deep lakes because of the winter drop in humidity in the overlying air, coupled with higher wind speeds and mass transfer in the air column. Furthermore, shorter-term fluctuations in evaporation are tied to like changes in wind speed and, to a lesser extent, net long-wave radiation. Not evident in Fig. 4 are the effects of individual events on evaporation. Although there is generally evaporation throughout the year, aside from a little condensation in May and June, large amounts of evaporation occur on an

episodic basis corresponding to high winds and dry air. Evaporation events occur on all lakes but are most pronounced on Lake Superior during the winter when cold dry air masses cross the lake quickly.

The major components of the Lake Ontario heat balance as calculated by the model are evident in Fig. 5. Similar figures for the other lakes are given in Appendix C. Incident short-wave radiation is the major input of energy to Lake Ontario ranging up to about 240 W m^{-2} for the monthly average (252 for Superior, 242 for Erie, 266 for St. Clair, and 274 for Huron, in Appendix C). Net long-wave radiation contributes about 7 W m^{-2} during the summer (43 for Superior and 37 for Erie). Net long-wave radiation throughout the rest of the year ranges up to 86 W m^{-2} outward (96 for Superior, 101 for Huron, 92 for St. Clair, and only 32 for Erie) and, together with evaporative and sensible heat transfers (up to 102 and 144 W m^{-2} outward respectively for Ontario, 106 and 199 for Superior, 97 and 149 for Huron, and 192 and 92 for Erie), represents the dominant losses. Although condensation occurs, it does not add much to the heat budget. Advection is very small and generally can be neglected on all lakes. During the winter, energy for the losses comes from the large heat storage built during the summer when wind-speed-controlled evaporation is lower. The total heat flux budget appears to close (there is no residual in the budget over the period 1950-1985) with as much outgoing energy as incoming energy over the annual cycle; since the average represents 36 years, little carryover is expected. Large residuals noted in earlier heat budgets (Schertzer, 1978), which are avoided only when evaporation is estimated as the heat budget residual, are minimized here by calibration of the flux models and heat storage function to best match surface temperatures.

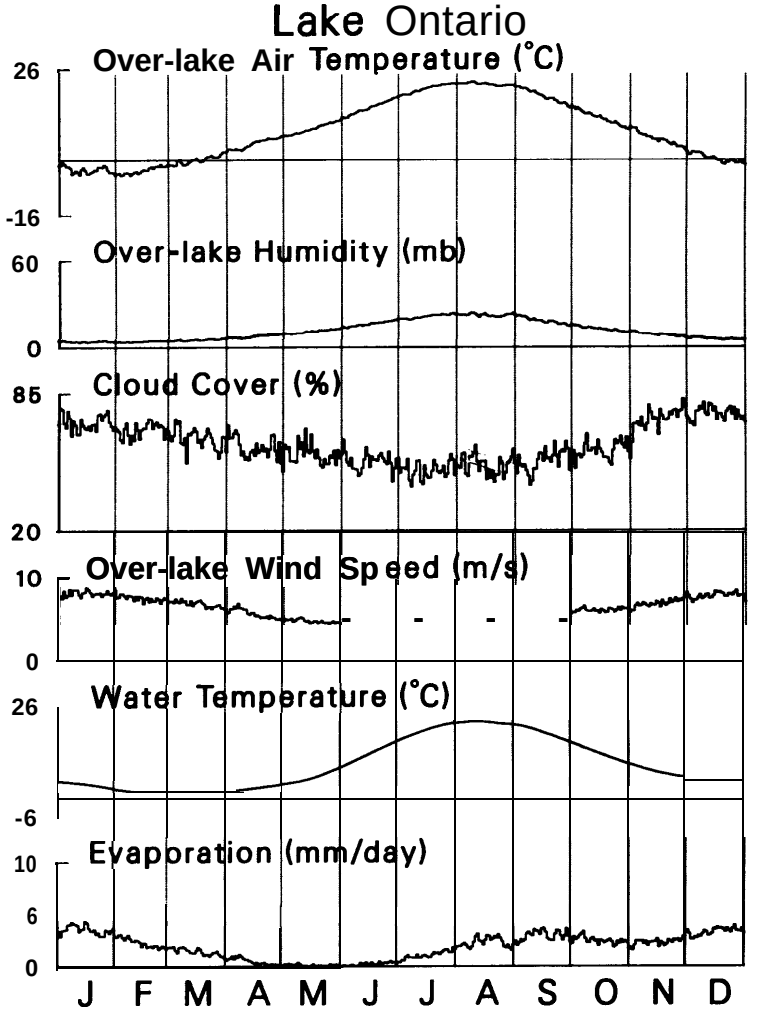

Figure 4.--Annual cycles of average Lake Ontario meteorology and evaporation.

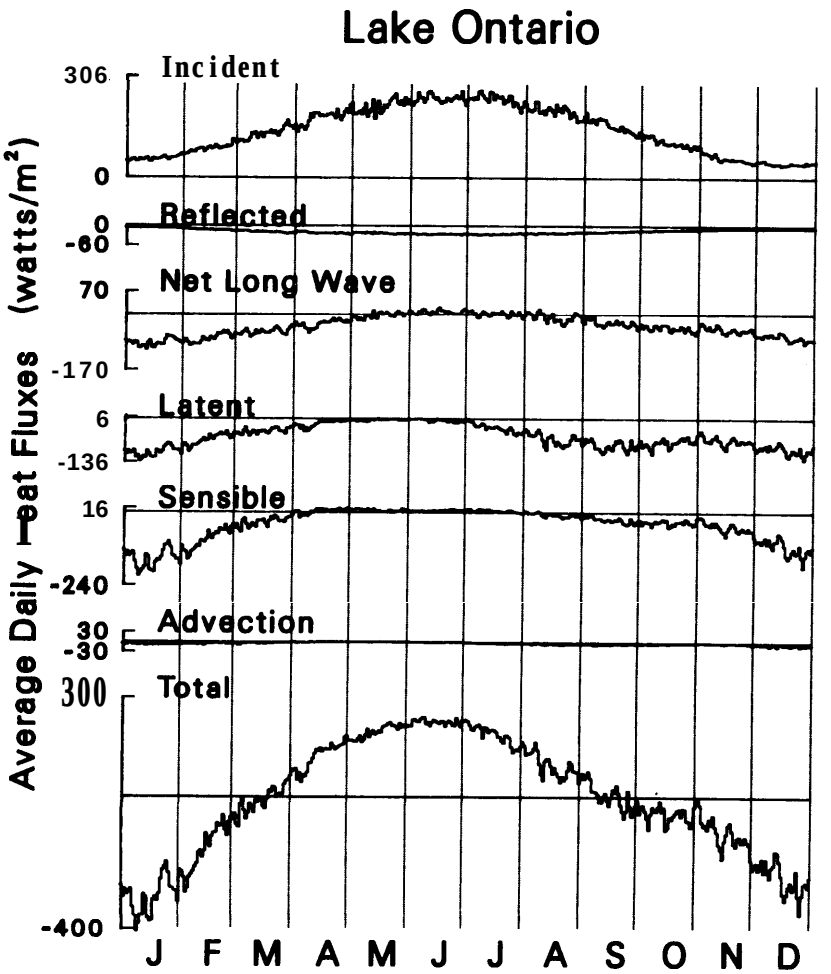

Figure K-Annual cycles of average Lake Ontario heat fluxes.

Figure 6 compares the model output for April 1972 through March 1973 (data wrap around the calendar year in Fig. 6) to Lake Ontario heat fluxes measured during IFYGL by Schertzer (Pinsak and Rodgers, 1981). Energy balances for several Great Lakes are documented elsewhere; Pinsak and Rodgers (1981) summarized two heat budgets on Lake Ontario during IFYGL (April 1972 - March 1973). Schertzer detailed the energy balance for Lakes Superior in 1973 (Schertzer, 1978) and Erie for 1967 to 1982 (Schertzer, 1987). The second data comparison for Lake Ontario and the comparisons for Superior and Erie are contained in Appendix D. The results are similar to those shown here. Although there is more variability in the daily estimates than in the weekly estimates in Fig. 6, the agreement is good. Sensible, latent, and net radiation are reasonably represented. The large peak in latent flux in July (and the corresponding peak in sensible flux) appears anomalous; it is not present in the estimate by Atwater (Pinsak and Rodgers, 1981). Several of the heat flux concepts used by Schertzer and Atwater (Pinsak and Rodgers, 1981; Schertzer, 1978, 1987) are similar to those used here, but all data used by these investigators are completely independent of those used here, representing independent estimates of the heat budget terms. Likewise, the total-flux comparisons in Fig. 6 and Appendix D are independent; the outside calculations of total flux proceeded as a residual when evaporation was estimated by means of a mass transfer method (Schertzer, 1987) and as a change in heat storage computation when temperature surveys with depth were available (Pinsak and Rodgers, 1981; Schertzer, 1978).

Figure 6 does not indicate the agreement of the components of the net radiation flux: incident, reflected, and longwave. These components are shown for other lakes in Appendices C and D, revealing that modeled net long-wave radiation is sometimes positive during the summer months on Lakes

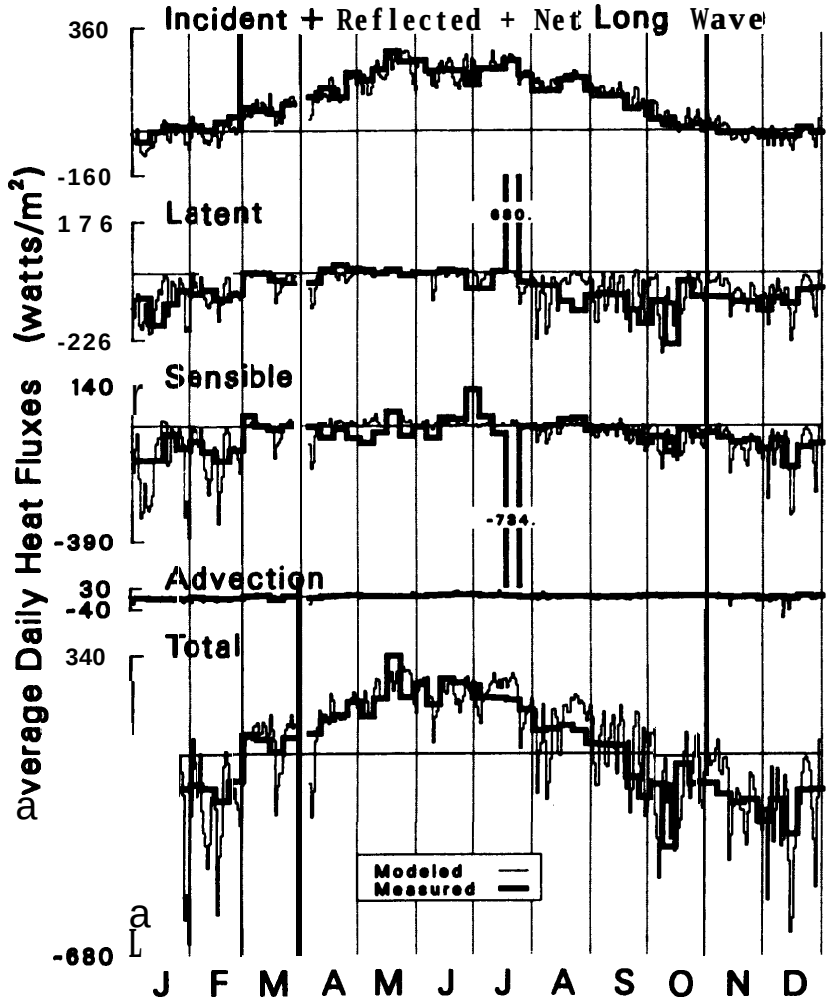

Figure 6.--Lake Ontario fluxes (April 1972-March 1973) from International Field Year for the Great Lakes.

Superior and Erie; that is long-wave radiation from the atmosphere to the lakes [first term in (33)] is then greater than long-wave radiation from the lake to the atmosphere [second term in (33)]. This is not in accord with current thinking for these lakes but may be the result of parameter compensation in the model calibrations; note that parameter p is higher on Lakes Superior and Erie. Keijman (1974) used p = 1.13 which is lower than that used here for any of the lakes. Perhaps atmospheric long-wave radiation is over estimated in the model to compensate for deficiencies in other modeled heat flux components. Further model analysis and consideration of measurements are necessary to understand the opportunity for parameter compensation in the model calibrations, the relevancy of the atmospheric long-wave radiation flux term in (33), and the omission of important concept components in the other heat budget terms in (29).

5.3 Water Balance Residuals

Water balance evaporation estimates were made to compare the evaporation estimates made previously with another approach and to indicate discrepancies in the water balance on any of the Great Lakes. Figure 7 presents the annual residual from a water balance on Lake Ontario (precipitation + runoff + inflows - outflows - evaporation - change in storage over the period) obtained by using evaporation estimated by the models presented herein and by using similar mass transfer evaporation models applied directly to the satellite-observed surface temperatures (without the heat balance and heat

storage models) as used operationally elsewhere (Atmospheric Environment Service, 1988). The former method is referred to in Fig. 7 and Appendix E as Croley and the latter method is referred to as Irbe. Residuals for the period 1965-85 are on the order of 50-150 $m^3 s^{-1}$. Compare this with an average flow through Lake Ontario of about 5500 $m^3 s^{-1}$; residuals represent about 1% to 3% of this flow and may be partially related to flow determination errors. Note that although the mass transfer evaporation equations are essentially the same, the use of observed water surface temperatures directly (Irbe) gives a larger residual 85% of the time than does the calibrated heat balance (Croley) in a water balance. Although it is difficult to discern where the errors are (they may be in the other water balance terms), it appears that the larger residual may result from errors in observed surface temperatures and data reductions that are filtered by the minimization of the root-mean-square error in the calibrations of the heat budget and heat storage models. Appendix E contains annual water balance residuals for the two methods for Lakes Superior, St. Clair, and Erie; a water balance for Lake Huron is not possible since reliable daily or monthly estimates of flow through the Straits of Mackinac are not available. Lake Superior residuals by Croley are on the order of 50 to 150 $m^3 s^{-1}$ whereas Irbe residuals are on the order of 75 to 300 $m^3 s^{-1}$; Irbe residuals exceeded Croley residuals for 80% of the years. It is surprising that both methods gave relatively large residuals on Lake Superior where there is less error in estimating the flows (there is no upstream inflow, and the outflow to the next Great Lake is the smallest in the system), but it may be related to improper consideration of the Ogoki diversion. This diversion ranges from about 100 to 250 $m^3 s^{-1}$ but is made into large Lake Nipigon, which releases its flow to Superior through a regulated channel. It is included in the water balance as part of the basin runoff to the lake, ignoring storage attenuation on Lake Nipigon. Its time of appearance on Lake Superior governs the size of the residual.

Lake St. Clair had very small annual residuals, generally less than 50 $m^3 s^{-1}$. No estimate of evaporation directly from surface temperatures is available for comparison. It is interesting to note that

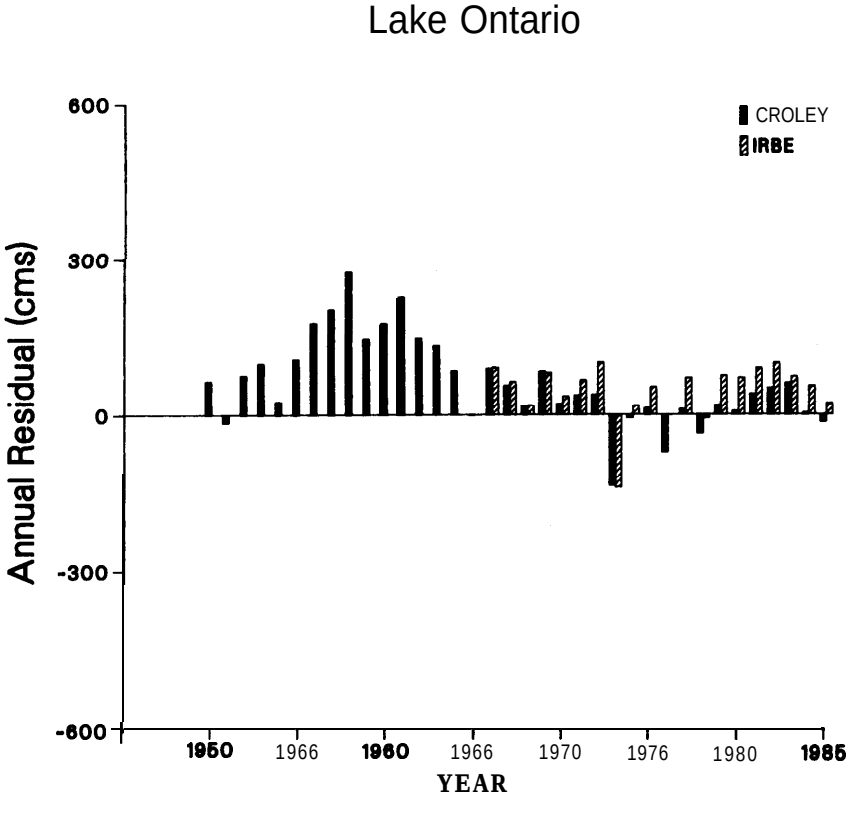

Figure 7.--Lake Ontario annual water balance residuals.

winter surface temperatures on Lake St. Clair are modeled poorly, yet the residual error appears small. This is largely because little evaporation occurs during the winter on Lake St. Clair because so little heat is stored in the lake.

Lake Erie showed annual residuals consistently negative on the order of 100 to 200 $m^3 s^{-1}$ for the evaporation model and consistently positive for the Irbe method, suggesting a problem with the estimation of evaporation or of mass balance components other than evaporation. Further analysis of the mass balance is required to assess the likelihood of such an error. In the earlier calibration, mentioned in section 5.1 (Calibration), where the evaporation mass transfer coefficient was allowed to float and the long-wave radiating temperature was taken as a linear function of the heat in storage, much better agreement with the Irbe evaporation estimates was observed in addition to a better match of satellite-observed surface temperatures. Although there is little physical basis for these extra degrees of freedom in the model, their net effect was to provide more heat release through long-wave radiation than through evaporation. The present model of Table 4 appears to overestimate evaporation, compared with mass-balance estimates or Irbe estimates. Part of the problem may be in poor estimates of other mass-balance components but the Irbe estimate and the Croley estimate should be close since the evaporation calculations are very similar. The difference might lie in the Irbe adjustment of satellite data to incorporate normal seasonal surface temperature variations, in the estimation of ice cover or over-water corrections, or in the use of different sets of meteorological stations (see Table 1).

Appendix E also contains seasonal average residuals for each month of the year. Those observations are similar to observations about annual residuals. Negative residuals on Lake Superior appear at the time of snowmelt and during the winter; positive residuals occur during the summer and fall. Lake Ontario seasonal residuals are negative in May, June, and July and then positive in the fall but small. They appear uncorrelated with evaporation on Lakes Superior and Ontario. Lake Erie seasonal residuals are large and negative but are closer to zero during the spring and maximum during the fall. Lake St. Clair seasonal residuals are almost zero throughout the annual cycle.

5.4 Model Sensitivities

To assess model sensitivity to the parameters, changes in the third significant digit (relative change of between 0.1% to 1.0%), both higher and lower, were made in each of the parameters, one at a time, from their calibrated values. Consequent changes in the root-mean-square error between actual and modeled temperatures and in the calculated evaporation were used to estimate those consequent with 1% parameter changes (Tables 5 and 6). Table 5 contains root-mean-square error changes and represents the sensitivity of the calibration to parameter fluctuations. Table 6 contains evaporation changes and represents the sensitivity of the evaporation estimate to parameter fluctuations.

Only increases in root-mean-square error were observed for parameter changes in any direction, of course, since the calibrations minimized this error and the parameter changes considered were small. All lakes are most sensitive to the cloud cover parameter p, since it governs the amount of incident long-wave radiation received. The lakes then appear sensitive to various heat storage parameters for the superposition model used during warm surface temperatures (above 3.98°C), particularly the exponent on temperature differences, c, on the deep lakes. Interpretation of these calibration sensitivities should be guarded since they represent the response surface only in the vicinity of the calibrated parameter values. These sensitivities appear differently about other sets of parameter values; this is illustrated somewhat by comparing the Lake Superior sensitivities and parameters with those in the other applications.

The sensitivity of the evaporation estimates to parameter changes in Table 6 reveals that evaporation also is most sensitive to the cloud cover parameter p, which controls the net long-wave radiation received. The sensitivity is fairly balanced with similar changes (inopposite directions) for parameter changes in both directions. It should-be noted that cloud cover estimates are also the most imprecise meteorological elements measured. Evaporation sensitivities to the heat storage parameters

Table 5.--Surface temperature RMSE rise for 1% parameter rises (drops) (°C)

Parameter	Lake				
	Superior	Huron	St. Clair	Erie	Ontario
a	**0.004 (0.005)**	**0.002** (0.001)	0.001 (0.002)	**0.004 (0.002)**	**0.000 (0.004)**
b	**0.003** (0.001)	0.001 (0.000)			**0.003 (0.001)**
c	**0.029 (0.008)**	**0.003 (0.003)**	o.ooo (0.001)	0.001 (0.001)	0.010 (0.004)
a'	0.001 (0.002)	o.ooo (0.000)	0.001 (0.000)	0.001 (0.000)	0.000 (0.006)
b'	0.001 (0.001)	o.ooo (0.000)	o.ooo	0.000	**0.000 (0.002)**
c'	**0.000 (0.008)**	**o.ooo (0.000)**	**0.008** (0.001)	0.001 (0.001)	0.000 (0.001)
P	**0.042 (0.008)**	**0.009 (0.015)**	0.011 (0.010)	**0.005 (0.004)**	**0.005** (0.018)

Table 6.--Evaporation rise for 1% parameter rises (drops) (cm yr^{-1})

Parameter	Lake				
	Superior	Huron	St. Clair	Erie	Ontario
a	-0.09 (0.04)	-0.11 (0.09)	**-0.06 (0.32)**	**-0.15 (0.13)**	-0.10 (0.09)
b	**-0.06 (-0.02)**	**-0.03 (0.02)**			**-0.02 (0.03)**
c	**0.05 (-0.25)**	0.11 (-0.25)	**0.25 (-0.02)**	**0.12 (-0.12)**	**0.22 (-0.09)**
a'	**-0.02 (-0.04)**	-0.01 (0.00)	**-0.27 (0.28)**	0.00 (0.03)	**-0.02 (-0.03)**
b'	0.00 (-0.03)	**0.00 (0.00)**	**0.00**	**0.00**	**0.02 (0.00)**
c'	**-0.03 (-0.12)**	0.00 (0.02)	**-0.88 (0.91)**	0.01 (0.02)	**0.03 (-0.02)**
P	1.07 (-1.09)	1.06 (-1.06)	1.44 (-1.43)	1.78 (-1.77)	1.29 (-1.28)

are similar in character to the calibration sensitivities in that their effects vary from lake to lake with the exception of parameter c. Small changes in this exponent can give large changes in heat storage per degree of temperature rise. The careful selection of this parameter allows mimicry of some aspects of the hysteresis present between heat in storage and surface temperature over the annual heating and cooling cycle. It appears that applications of the heat balance, heat storage, and evaporation models described here to other deep lakes for which surface temperatures are not available, such as Lake Michigan, will require careful selection particularly of a, c, and p and generally of b, a', b', and c'.

6. SUMMARY

Remotely-sensed water surface temperatures make it possible to calibrate a joint evaporation - **heat** balance - heat storage model; such calibrations are not possible in terms of matching measured evaporation since independent evaporation estimates do not exist for the Great Lakes or are too crudely determined in energy or water balances. Traditional **heat** flux expressions are combined with current USC

of the aerodynamic (evaporation) equation, mass transfer coefficients being determined from stability considerations and used with a new lumped model of heat storage in a lake. This makes it possible to model surface temperature as well as evaporation, which makes the model amenable to use in settings where surface temperatures are unknown, including forecasts, climate change simulations, and assessments of management impacts on the hydrology of the Great Lakes.

The heat storage model is a superposition model in which the latest heat additions to the lake are the first removed. Although, conceptually, heat losses actually come from some mix of past heat additions, this model allows aging of heat additions to be considered that describe well the observed hysteresis between stored heat and surface temperature. Alternate aging functions, perhaps as functions of wind history, may better describe the maturation of the heat distribution in a lake and this is an area for future research with lumped heat storage models.

The new heat storage model, when used with contemporary treatments of evaporation and heat exchange, appears to do a good job of replicating average area1 surface temperatures and heat fluxes on the deep lakes. Correlations between model and satellite-observed average area1 surface temperatures are 0.97-0.99 during the calibration period of 1979-85 and range from 0.93-0.98 during a verification period of 1966-78. The corresponding root-mean-square errors are 1.2-l .5°C for the calibrations and 1.3-1.6°C for the verification periods on the deep lakes. These errors compare favorably with reported accuracies for reduction of satellite data. On the shallow lakes, greater errors in surface temperature are observed in the calibrations. On Lake Erie, it appears that resulting evaporation may also be overestimated. Future research can address alternate heat flux formulations, wind-induced mixing (aging) functions, and heat storage models more appropriate for shallow lakes. Inspection of model outputs reveals that significant aspects of the annual heating and cooling cycle in each Great Lake are replicated, including the spring and fall turnovers, near-peak daily average surface temperatures, and above-freezing winter surface temperatures. Resulting heat fluxes agree very well with independent data sets used by other investigators, where available, for Lakes Superior, Erie, and Ontario, with the possible exception of atmospheric long-wave radiation; further work is necessary to see if overestimation of this exists and results from parameter compensation in the model calibrations and then to see what other terms are being compensated.

The use of these evaporation estimates in water balances for each of the lakes reveals that there are water balance residuals. These residuals are largest on Lake Erie and may be related to neglected water balance terms (such as groundwater), systematic errors of measurement of river inflows and outflows and runoff, and/or process model errors in the evaporation. This is an area for further research, because these residuals must be considered for simulations of climate change or management impacts on lake levels or for forecasting of lake levels. Although the nature of the residuals is unresolved at present, comparisons with conventional evaporation models that use observed surface temperatures directly indicate that the residuals are reduced by considering the heat exchange and heat storage in each deep lake.

Other areas for further research include improvements to the models in the areas of ice-cover estimation, incorporation of better ice-cover thermodynamics into the heat balance, estimation of ice-cover effects on heat fluxes (notably long-wave exchange and reflection), and better assessment of over-water corrections to over-land meteorology.

7. REFERENCES

ASSEL, R.A. A computerized ice concentration data base for the Great Lakes. NOAA DR ERL GLERL-24 (PB83-233031), 20 pp. (1983a).

ASSEL, R.A. Lake Superior bathythermograph data: 1973-79. NOAA DR ERL GLERL-25 (PB83-252890), 17 pp. (1983b).

ASSEL, R.A. Lake Superior cooling season temperature climatology. NOAA TM ERL GLERL-58 (PB86-110624/XAB), 45 pp. (1985).

Atmospheric Environment Service. Monthly and annual evaporation from the Great Lakes bordering Canada, Environment Canada, Atmospheric Environment Service, Downsview, Ontario, Canada (1988).

Bennett, E.B. Water budgets for Lake Superior and Whitefish Bay. Journal of Great Lakes Research 4(3-4):331-342 (1978a).

Bennett, E.B. Characteristics of the thermal regime of Lake Superior. Journal of Great Lakes Research 4(3-4):343-354 (1978b).

BOLSENGA, S.J. Estimating energy budget components to determine Lake Huron evaporation. Water Resources Research 11(5):661-666 (1975).

Businger, J.A. Transfer of momentum and heat in the planetary boundary layer. Proceedings, Symposium Arctic Heat Budget and Atmospheric Circulation, The RAND Corporation, 305-331 (1966).

Chamock, H. Wind stress on a water surface. Quarterly Journal of the Royal Meteorological Society 81:639-640 (1955).

CROLEY, T.E., II, and H.C. HARTMANN. Lake Superior basin runoff modeling. NOAA TM ERL GLERL-50 (PB84-230028), 294 pp. (1984).

Davies, J.A., and W.M. Schertzer. Canadian radiation measurements and surface radiation balance estimates for Lake Ontario during IF'YGL. IFYGL Project Nos. 71EB and 80EB, Contract No. OSP3-0017, Canada Centre for Inland Waters, Burlington, Ontario, Canada (1974).

DERECKI, J.A. Multiple estimates of Lake Erie evaporation. Journal of Great Lakes Research 2(1):124-149 (1976a).

DERECKI, J.A. Heat storage and advection in Lake Erie. Water Resources Research 12(6):1144-1150 (1976b).

DERECKI, J.A. Evaporation from Lake St. Clair. NOAA TM ERL GLERL-23 (PB295686/OGA), 34 pp. (1979).

DERECKI, J.A. Estimates of Lake St. Clair evaporation. Journal of Great Lakes Research 5(2):216-220 (1979).

DERECKI, J.A. Stability effects on Great Lakes evaporation. Journal of Great Lakes Research 7(4):357-362 (1981a).

DERECKI, J.A. Operational estimates of Lake Superior evaporation based on IFYGL findings. Water Resources Research 17(5):1453-1462 (1981b).

Dyer, A.J. A review of flux-profile relationships. Boundary Layer Meteorology 7:363-372 (1974).

Gill, A.E., and J.S. Turner. A comparison of seasonal thermocline models with observation. Deep-Sea Research 23:391-401 (1976).

Gray, D.M., G.A. McKay, and J.M. Wigham. Energy, evaporation, and evapotranspiration. In Handbook on the Principles of Hydrology, D.M. Gray (ed.). Water Information Center, New York, 3.1-3.66 (1973).

Hicks, B.B. Reply. Boundary Layer Meteorology 10:237-240 (1976).

Irbe, J.G., and A. Saulesleja. An operational program for monitoring surface temperatures of lakes and coastal-zone waters in Canada from polar-orbiting satellite infrared data. Actes du symposium international de la Commission VII de la Societe intemationale de photogrammetrie et teledetection, 13-17 September, Toulouse, France, International Archives of Int. Soc. Photogram. and Remote Sensing 24(VII-1):717-724 (1982).

Irbe, J.G., R.K. Cross, and A. Saulesleja. Remote sensing of surface water temperature of the Great Lakes and off the Canadian east coast. Northwest Atlantic Fisheries Organization Scientific Council Studies No. 4, Special Session on Remote Sensing, September, Dartmouth, Canada, 31-39 (1982).

Irbe, J.G. An operational program for measuring surface water temperature by airborne radiation thermometer [ART] survey. Proceedings, First Canadian Symposium on Remote Sensing, Atmospheric Environment Service, Department of the Environment, 183-200 (1972).

Keijman, J.Q. The estimation of the energy balance of a lake from simple weather data. Boundary-Layer Meteorology 7:399-407 (1974).

Kramer, C. Computation of the mean evaporation for various parts of the Netherlands according to Penman's method. Kon. Ned. Meteor., Inst., Med. Verh. 70, (1957).

Kraus, E.B., and J.S. Turner. A one-dimensional model of the seasonal thermocline II; the general theory and its consequences. Tellus 19:98-105 (1967).

Panofsky, H.A. Determination of stress from wind and temperature measurements. Quarterly Journal of the Royal Meteorological Society 89:85-94 (1963).

Paulson, C.A. The mathematical representation of wind speed and temperature profiles in the unstable atmospheric surface layer. Journal of Applied Meteorology 9:857-861 (1970).

Penman, H.L. Natural evaporation from open water, bare soil and grass. Proc. Roy. Soc. London A193:120-145 (1948).

Phillips, W.D. Evaluation of evaporation from Lake Ontario during IFYGL by a modified mass transfer equation. Water Resources Research 14((2):197-205 (1978).

Phillips, W.D., and J.G. Irbe. Land-to-lake comparison of wind, temperature, and humidity on Lake Ontario during the International Field Year for the Great Lakes (IFYGL). Rep. CLI-2-77, Environment Canada, Atmospheric Environment Service, Downsview, Ontario, Canada (1978).

Pinsak, A.P., and G.K. Rodgers. Energy balance. In IFYGL - The International Field Year For The Great Lakes, E.J. Aubert and T.L. Richards (eds.). National Oceanic and Atmospheric Administration, Great Lakes Environmental Research Laboratory, Ann Arbor, MI, 169-197 (1981).

QUINN, F.H. An improved aerodynamic evaporation technique for large lakes with application to the International Field Year for the Great Lakes. Water Resources Research 15(4):935-940 (1979).

QUINN, F.H. and R.K. KELLEY. Great Lakes monthly hydrologic data. NOAA DR ERL GLERL-26 (PB84-114545), 87 pp. (1983).

Richards, T.L, and J.G. Irbe. Estimates of monthly evaporation losses from the Great Lakes, 1950 to 1968 based on the mass transfer technique. Paper presented at the 12th Conference on Great Lakes Research, International Association of Great Lakes Research, Ann Arbor, Michigan, May, 1969 (unpublished).

Schertzer, W.M. Energy budget and monthly evaporation estimates for Lake Superior, 1973. Journal of Great Lakes Research 4(3-4):320-330 (1978).

Schertzer, W.M. Heat balance and heat storage estimates For Lake Erie, 1967 to 1982. Journal of Great Lakes Research 13(4):454-467 (1987).

Smith, S.D., and E.G. Banke. Variation of sea surface drag coefficient with wind speed. Quarterly Journal of the Royal Meteorological Society 101:665-673 (1975).

U.S. Geological Survey. Water loss investigations, Vol. 1, Lake Hefner studies. Geological Survey Professional Paper 269 U.S. (1954).

U.S. Geological Survey. Water loss investigations: Lake Mead studies, Geological Survey Professional Paper 298 U.S. (1958).

Webb, E.K. Profile relationships, the log-linear range, and extension to strong stability. Quarterly Journal of the Royal Meteorological Society 96:67-90 (1970).

8. NOTATION

A = area of the lake surface
A(Z) = area of water surface at height Z
a = empirically derived heat storage parameter, $T_w > 3.98°C$.
a' = empirically derived heat storage parameter, $T_w \leq 3.98°C$.
a_1, a_2 = empirical coefficients for bulk evaporation
a_3, a_4 coefficient determination
B = the Bowen ratio
B' = the Bowen ratio over ice
b = empirically derived heat storage parameter, $T_w > 3.98°C$.
b = empirically derived heat storage parameter, $T_w \leq 3.98°C$.
C = specific heat of water
CE = the bulk evaporation coefficient
CH = the sensible heat coefficient
C_p = specific heat of air at constant temperature
c = empirically derived heat storage parameter, $T_w > 3.98°C$.
c' = empirically derived heat storage parameter, $T_w \leq 3.98°C$.
c_1, c_2 & c_3 = empirical ice coefficients on monthly air temperature
D = over-water dew point temperature
D_l = over-land dew point temperature
d = time in one day
E_i = evaporation over ice
E_w = evaporation over water
e_a = the vapor pressure of the atmosphere at the 2-m height
e_w = saturation water vapor pressure at T_w
f = the heat of fusion for water
g = acceleration due to gravity
H = the heat delivered to the ice cover each day
H_d = heat in storage at turnover
H_j = heat in storage in the lake at the end of day j
I = monthly average fraction of the surface covered by ice
I_b = fraction of the ice that is bare of snow
I_m = fraction of the ice covered with melting snow

I_n = fraction of the ice covered with new snow
I_o = fraction of the ice covered with old snow
k = von Kármán's constant
L = Monin-Obukhov length
M_1 & M_2 = the masses of the ice cover at the beginning and end of the day, respectively
N = cloud cover expressed as a fraction
0 = river outflow rate from the lake
o = neglected terms in heat balance for a lake
o′ = neglected terms in the ice cover heat balance
P = precipitation rate expressed as a depth per unit time
P_a = atmospheric pressure
P = an empirical coefficient that reflects the effect of cloudiness on the atmospheric long-wave radiation to the Earth
Q = turbulent heat flux
QI = daily average rate of energy advection into a lake by runoff and river inflow
QO = daily average rate of energy advection out of a lake
QP = daily average rate of energy advection into a lake by precipitation on a unit surface area
$Q_{P'}$ = daily average rate of energy advection onto a unit surface area by precipitation on the ice
Q_d = daily average rate of long-wave radiation from the atmosphere to a unit surface area
Q_e = daily average rate of evaporative and sensible heat transfers from a unit water surface area
Qe = daily average rate of evaporative and sensible heat transfers from a unit ice surface area
Qi = daily average rate of incident short-wave radiation to a unit surface area
Q_l = daily average rate of net long-wave radiation exchanged between the atmosphere and a unit water surface area
Q i = daily average rate of net long-wave radiation exchanged between the atmosphere and a unit ice surface area
Qm = correction to heat balance for the disappearance of the ice cover during the day
Qr = daily average rate of short-wave radiation reflected from a unit water surface area
Q r = daily average rate of short-wave radiation reflected from a unit ice surface area
Q_u = daily average rate of long-wave radiation from a unit surface area
QO = daily average short-wave radiation rate received on a horizontal unit area of the Earth's surface under cloudless skies
q = specific humidity of the atmosphere
q_w = saturation specific humidity at the surface temperature
R = runoff from the basin to the lake and river flow rates to the lake
r = air density
r_i = density of ice
r_w = density of water
S_1 = stability-dependent parameter for the wind profile
S_2 = stability-dependent parameter for the temperature profile
T = potential temperature at reference height
T_* = a scaling temperature
T_a = over-land air temperature
T_a' = absolute air temperature (kelvins)
T_d = temperature of maximum water density
T_j = surface temperature (T_w) at the end of day j
T_w = potential temperature at Z_w
Υ = absolute temperature of near-surface air
Υ_a = average monthly over-land air temperature
$\Upsilon_{a\text{-}l}$ = average monthly over-land air temperature for previous month
U = mean wind speed at reference height Z above the surface
U_* = friction velocity

v = the latent heat of vaporization
v' = the latent heat of vaporization evaluated at the temperature of the ice
W = over-land wind speed
x = empirically derived parameter
x' = empirically derived parameter
y = heat penetration depth below water surface
Z = reference height above water surface
Z_w = roughness length

Appendix A: Great Lakes Water Surface Temperatures

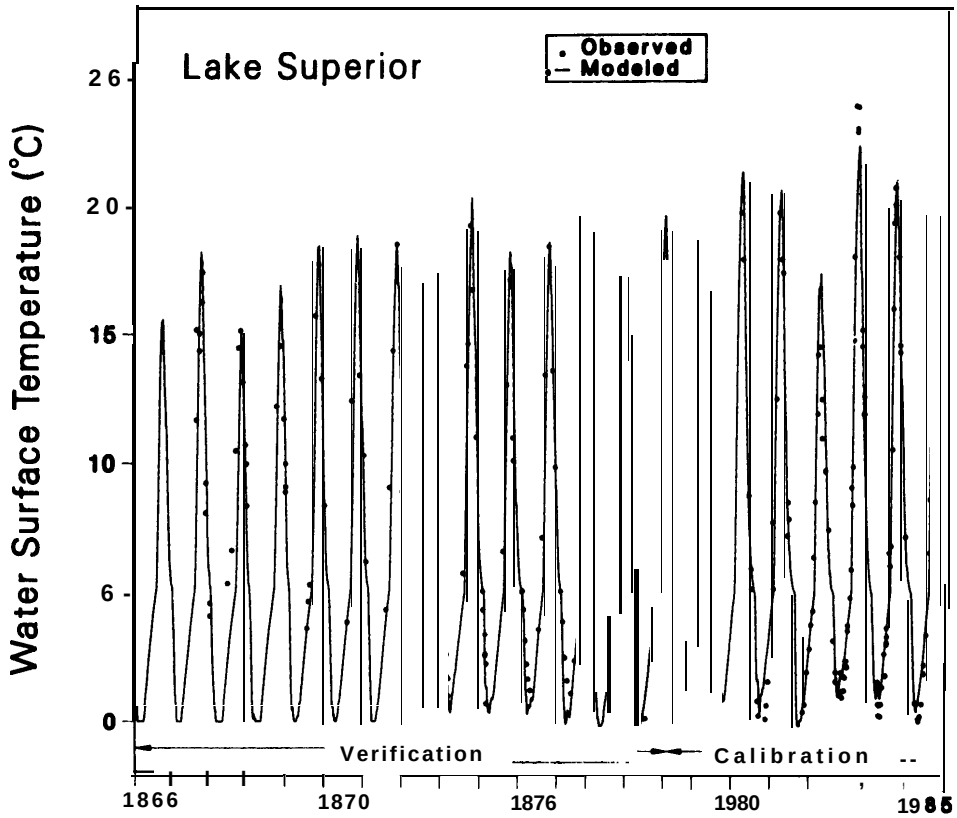

Figure A.1.--Lake Superior water surface temperature.

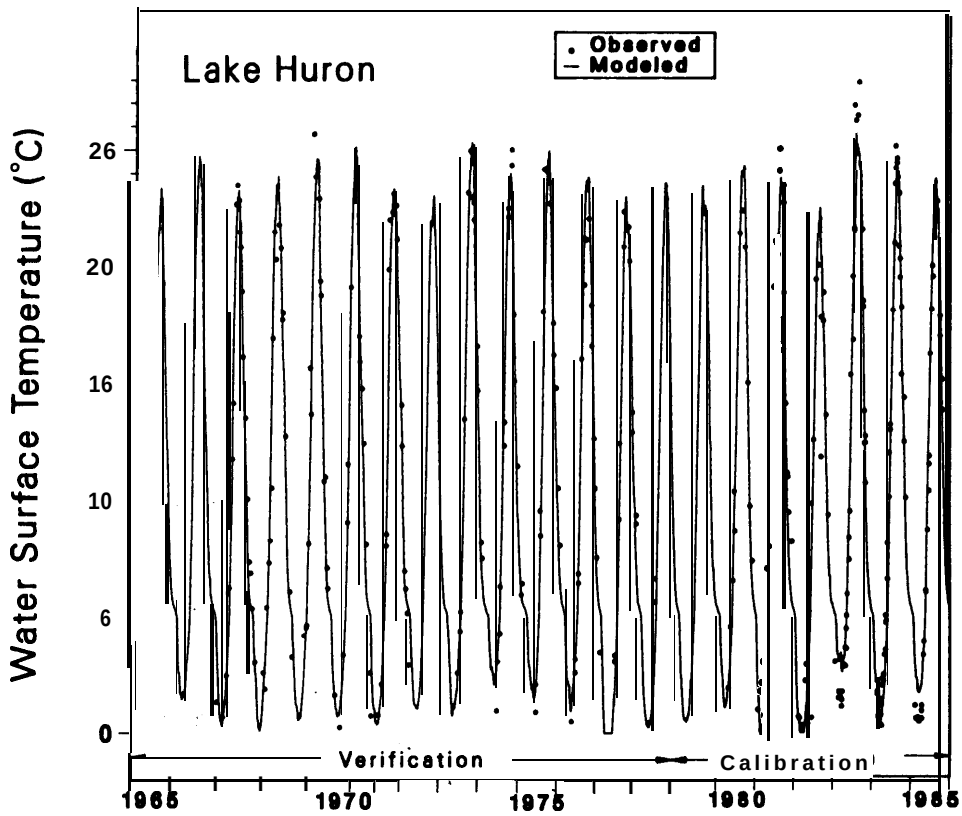

Figure A.2.--Lake Huron water surface temperature.

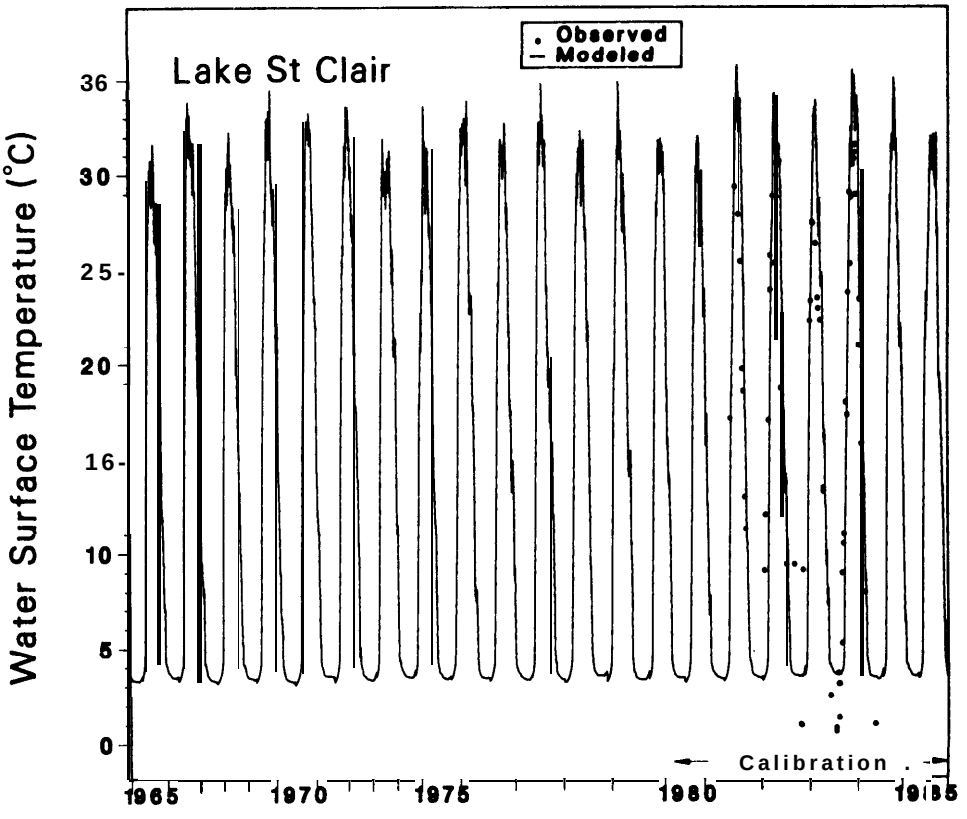

Figure A.3.--Lake St. Clair water surface temperature.

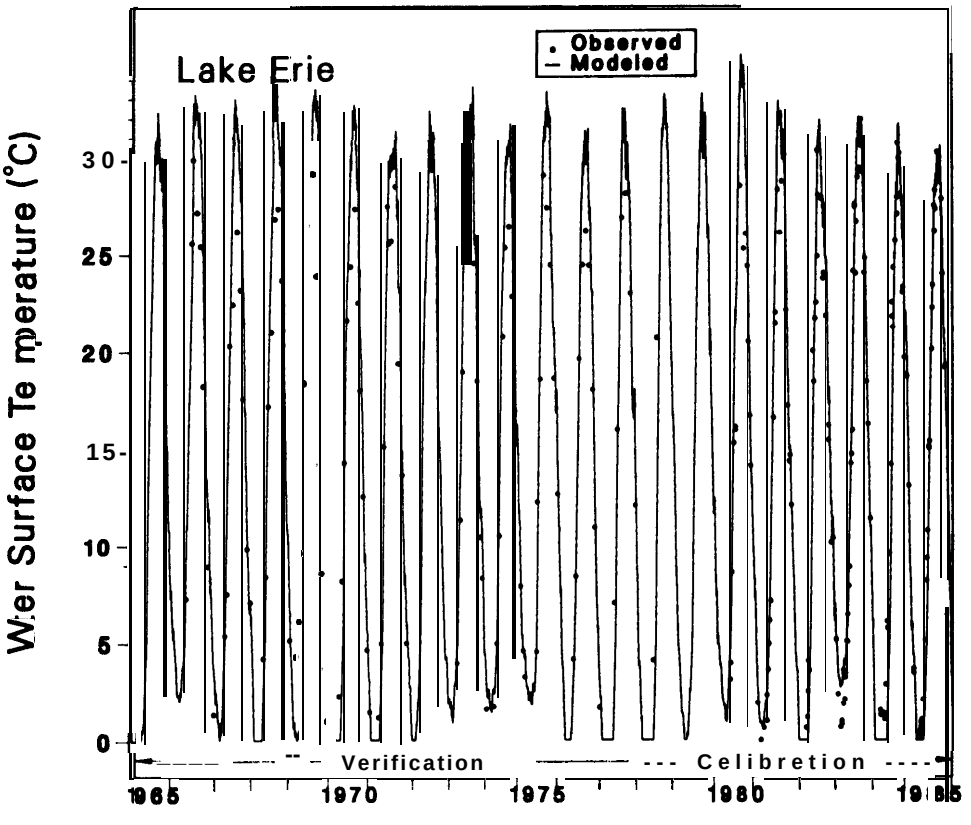

Figure A.4.--Lake Erie water surface temperature.

Appendix B: Annual Cycles of Average Great Lakes Meteorology and Evaporation

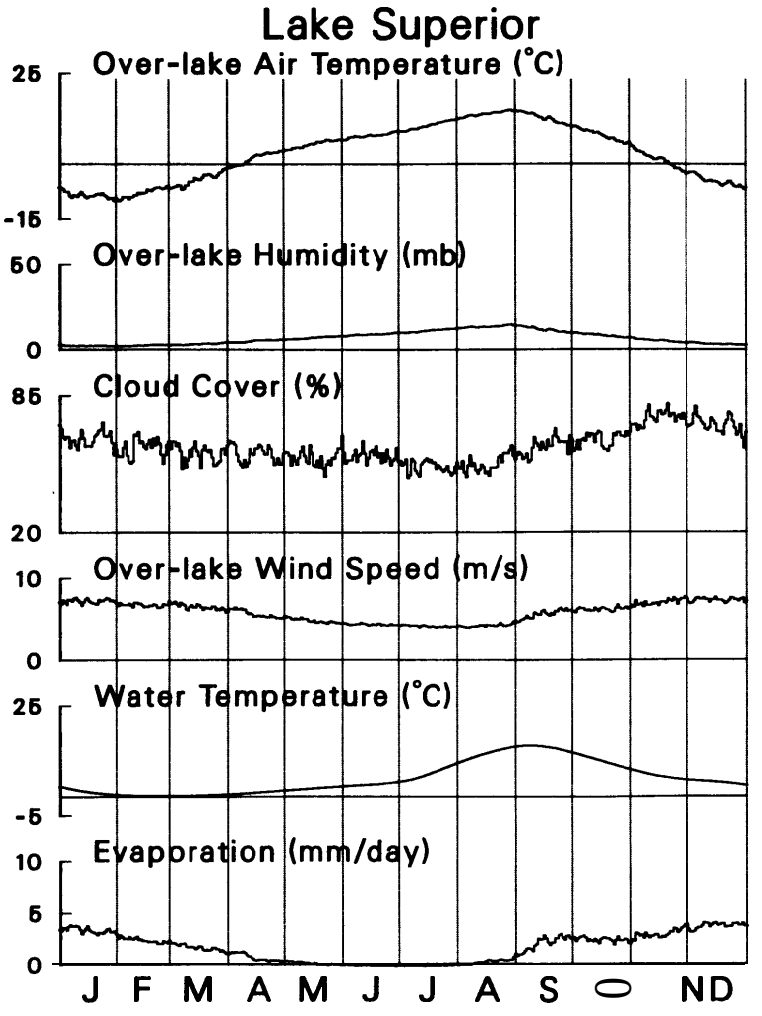

Figure B.1.--Annual cycles of average Lake Superior meteorology and evaporation.

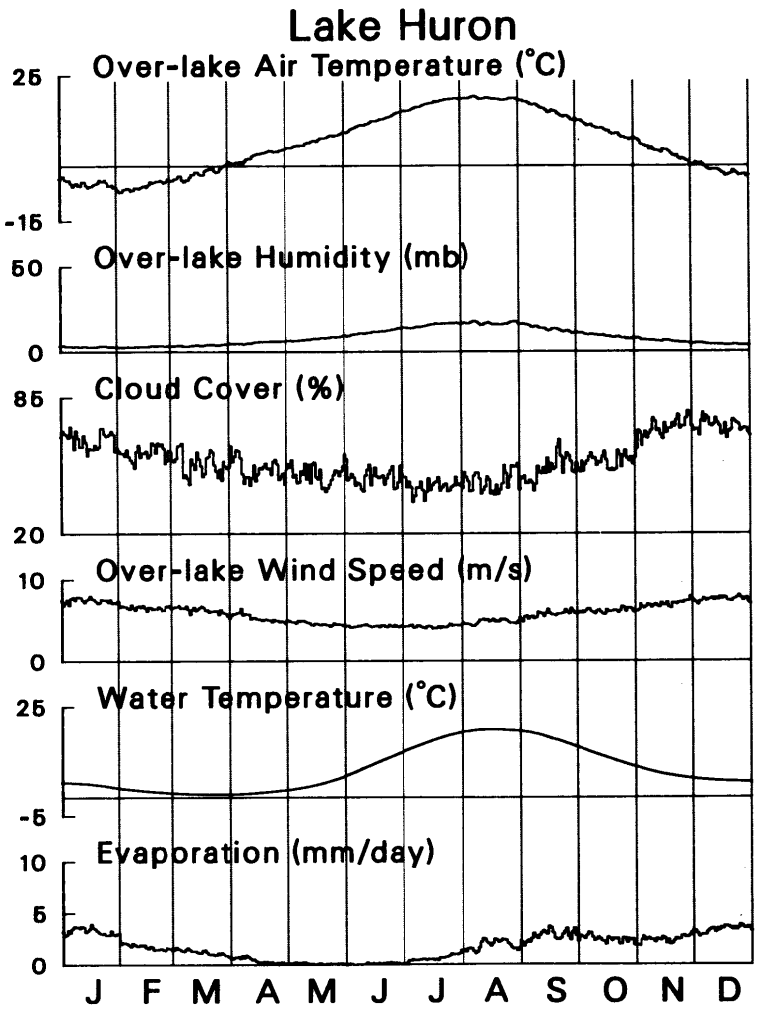

Figure B.2.--Annual cycles of average Lake Huron meteorology and evaporation.

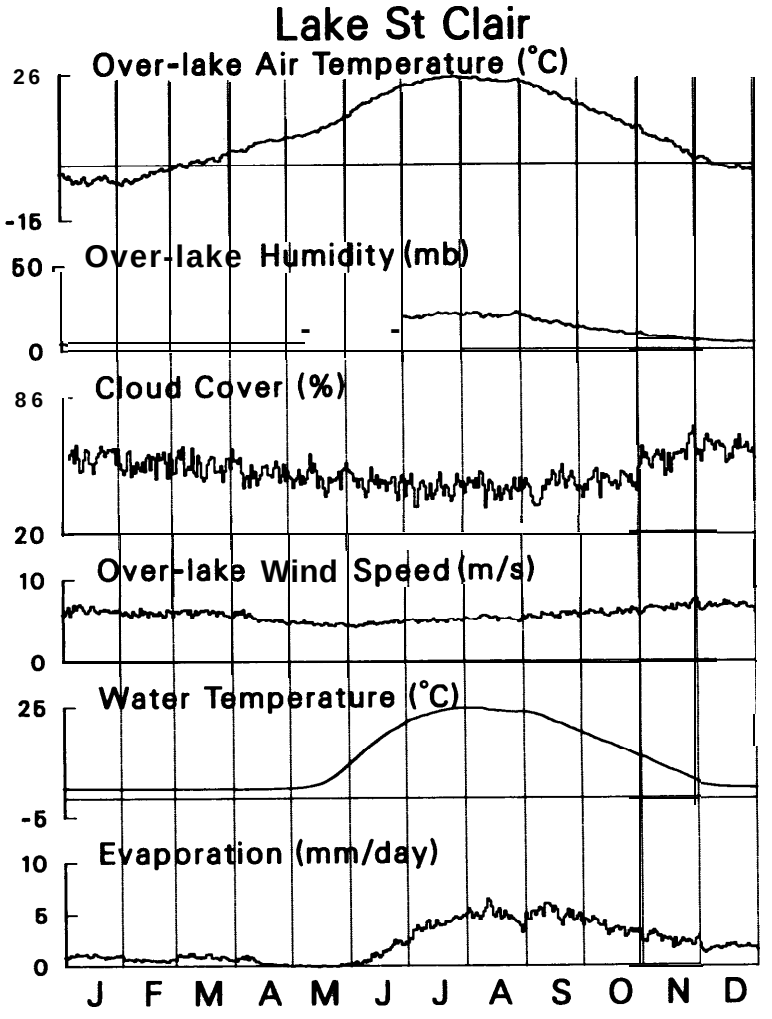

Figure B.3.--Annual cycles of average Lake St. Clair meteorology and evaporation.

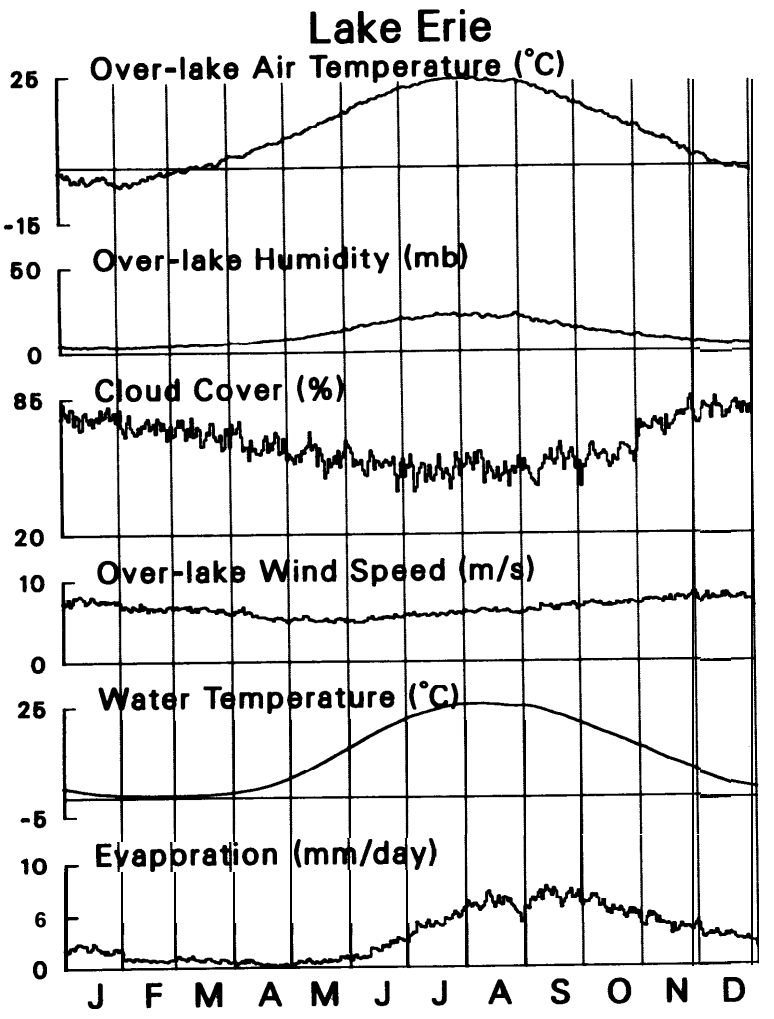

Figure B.4.--Annual cycles of average Lake Erie meteorology and evaporation.

Appendix C: Annual Cycles of Average Great Lake Heat Fluxes

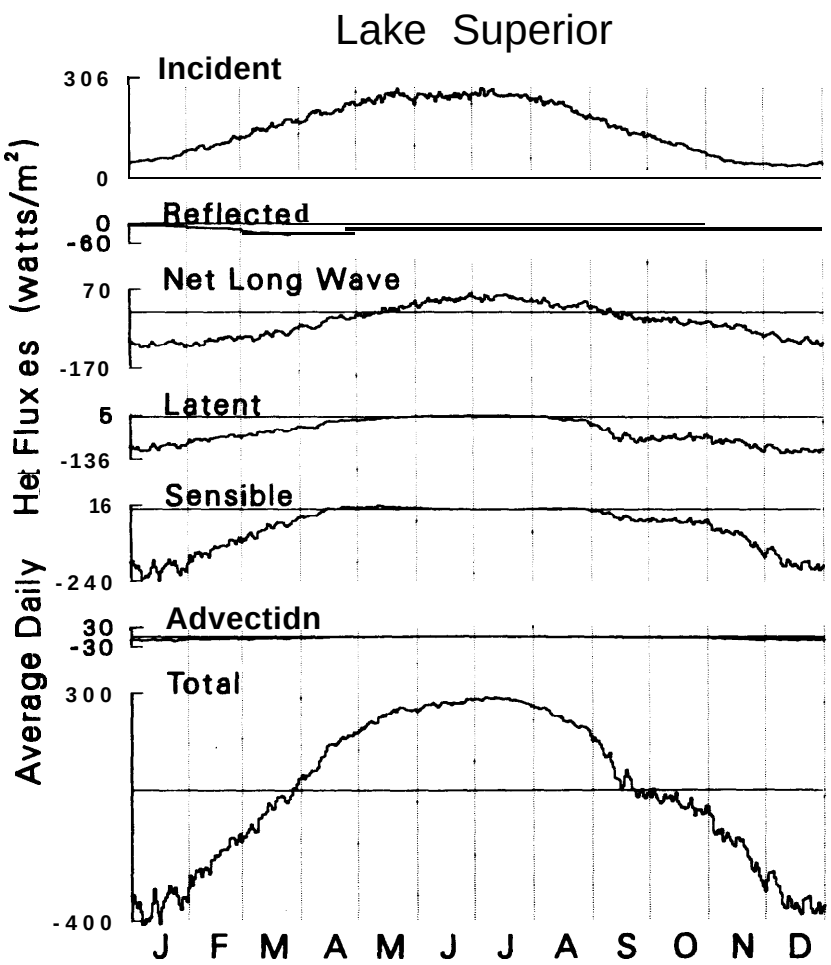

Figure CL--Annual cycles of average Lake Superior heat fluxes.

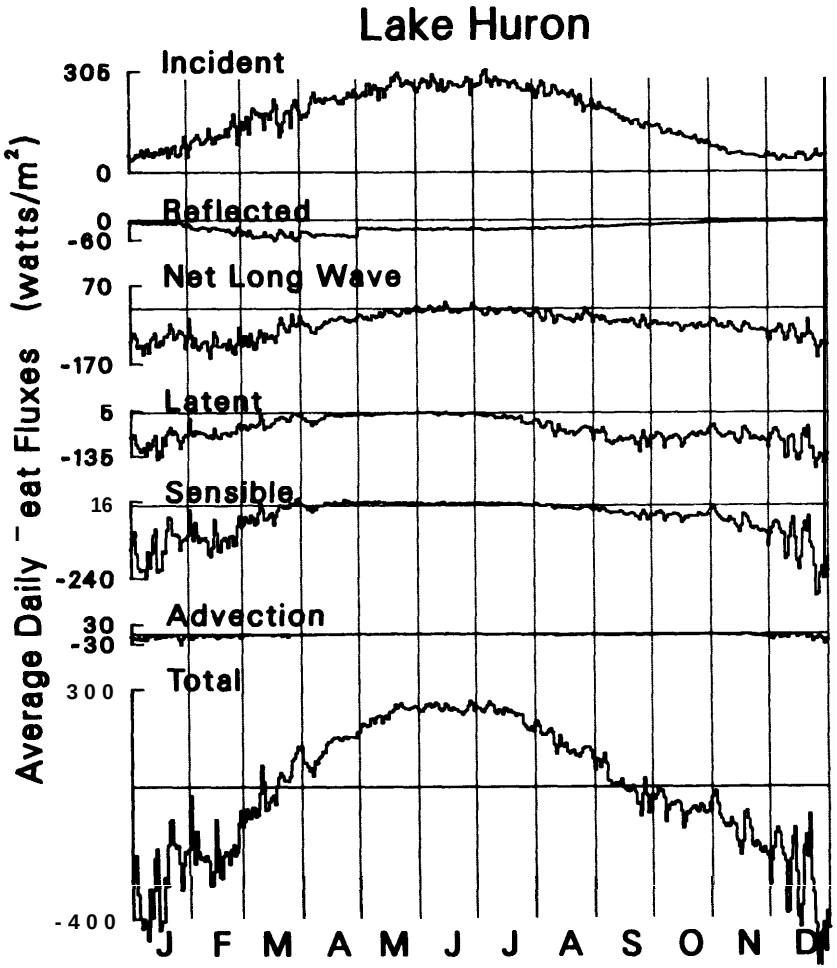

Figure C.2.--Annual cycles of average Lake Huron heat fluxes.

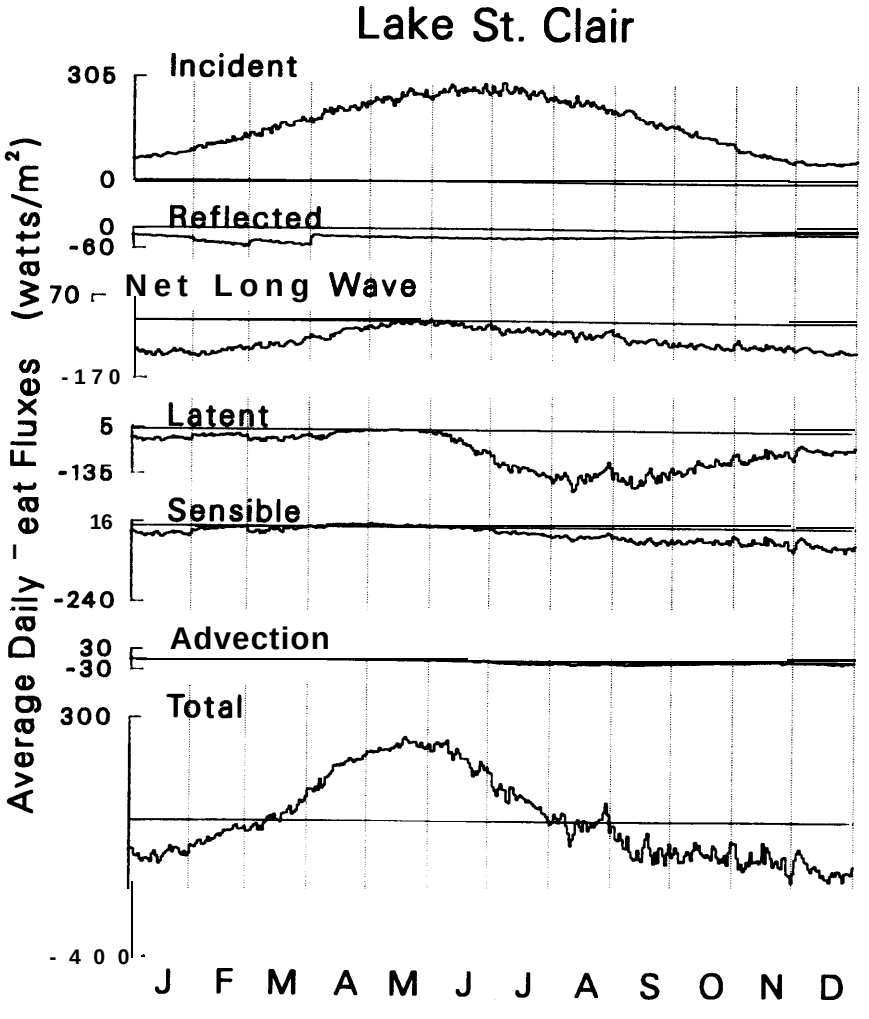

Figure C.3.--Annual cycles of average Lake St. Clair heat fluxes.

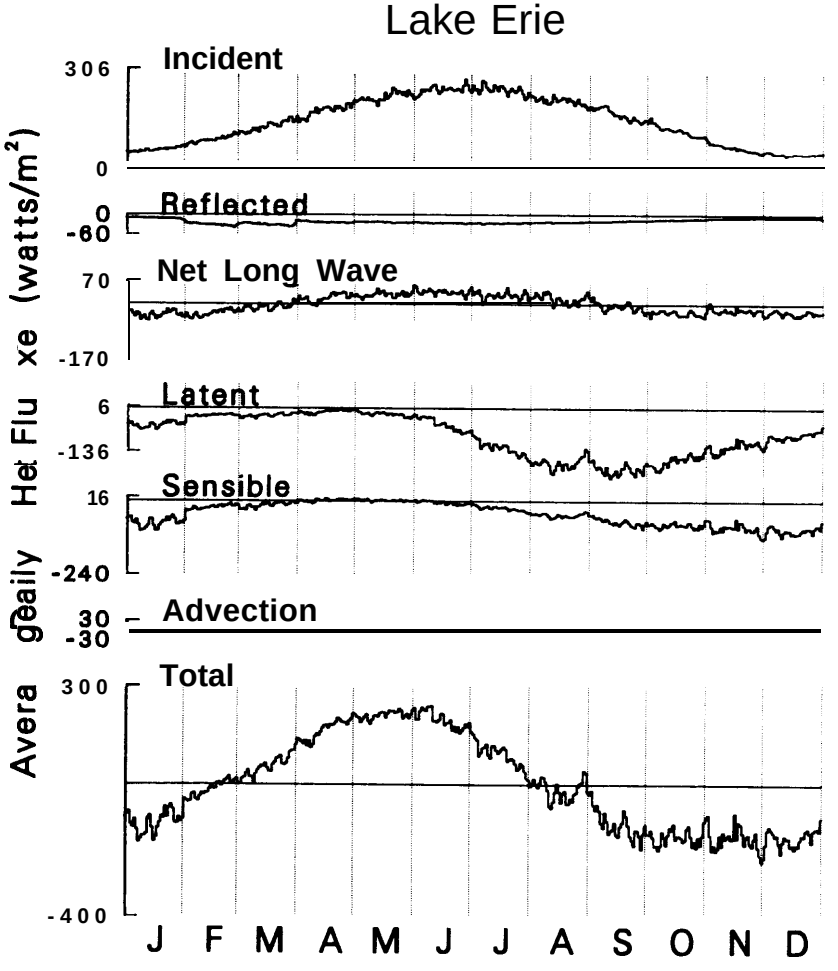

Figure C.4.--Annual cycles of average Lake Erie heat fluxes.

Appendix D: Comparisons of Great Lake Energy Fluxes

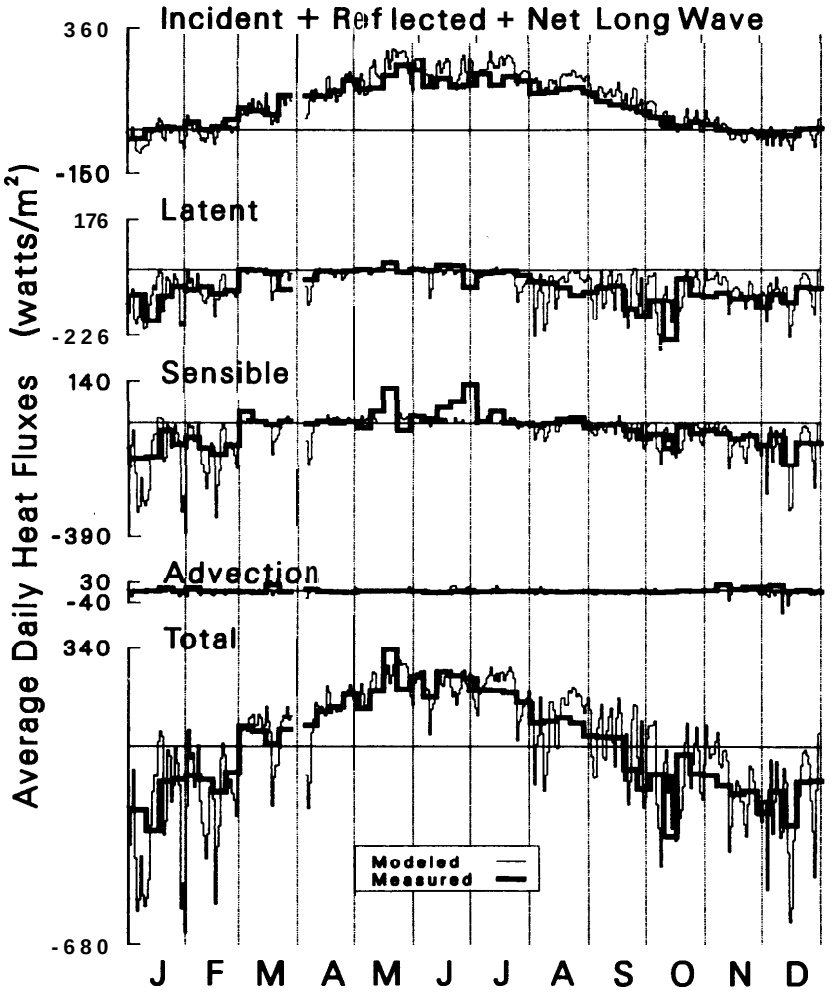

Figure D.1.--Lake Ontario fluxes (April 1972-March 1973) from International Field Year for the Great Lakes (Atwater; see Pinsak and Rodgers, 1981).

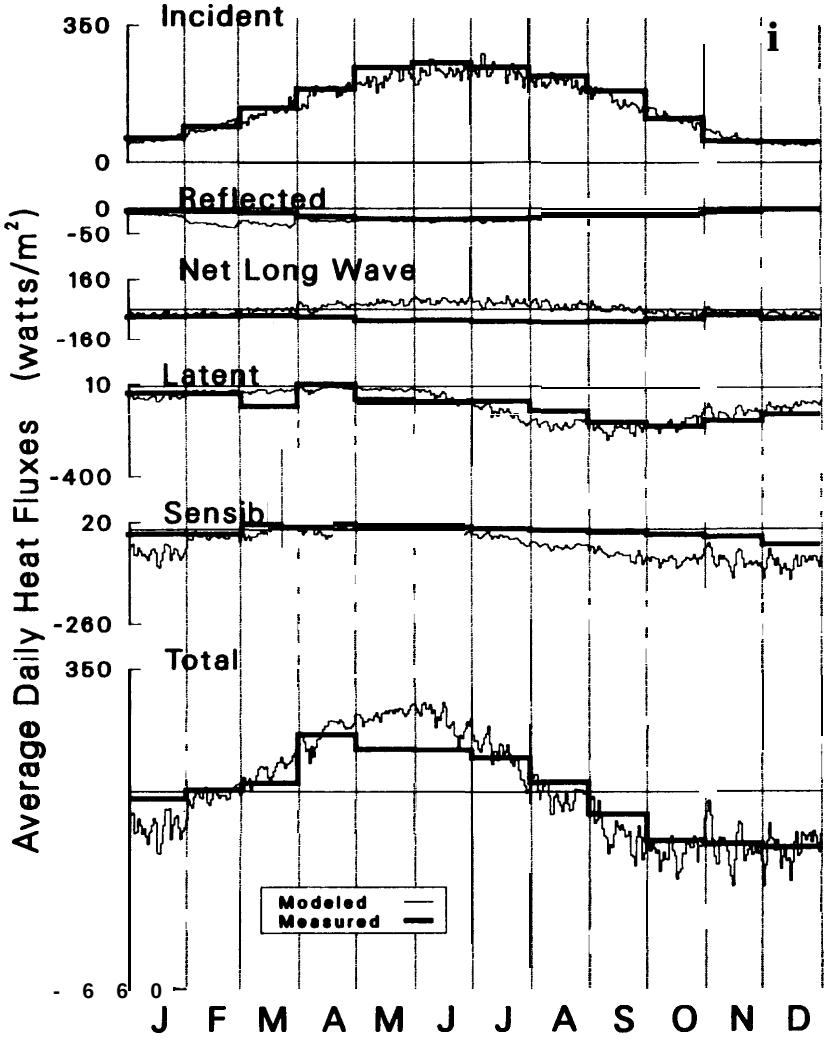

Figure D.2.--Lake Erie fluxes (April-November 1967432 and December-March 1952-1968) Lake Erie fluxes comparison (Schertzer, 1987).

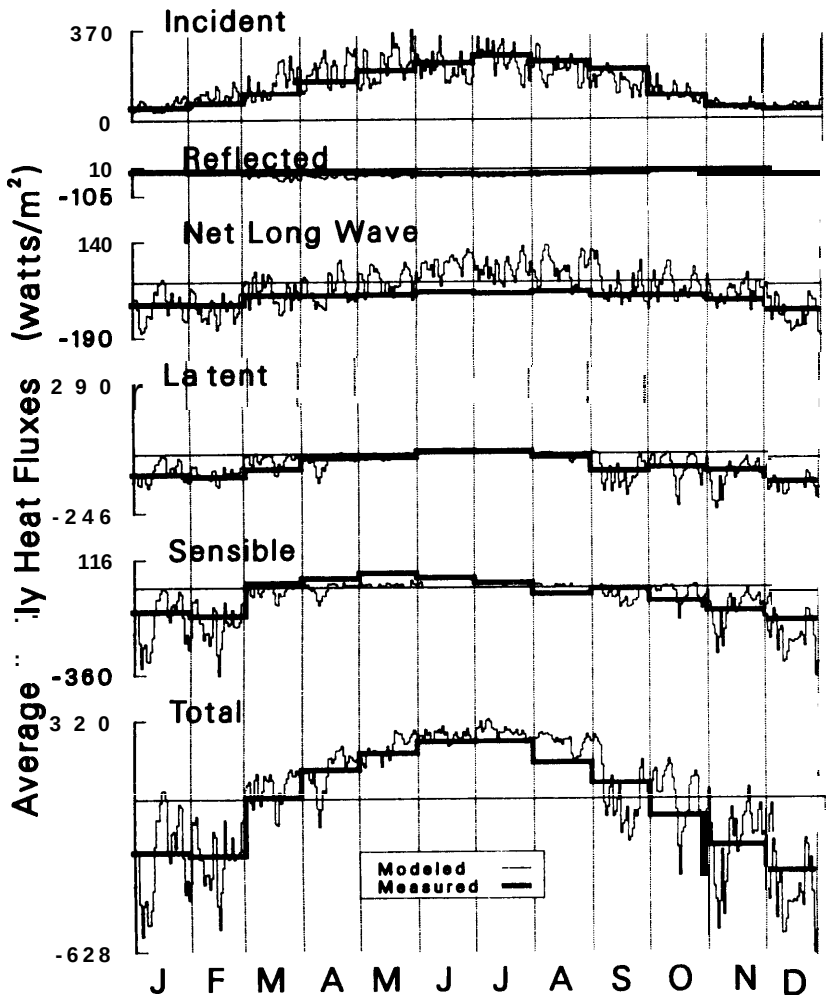

Figure D.3.--1973 Lake Superior fluxes (Schertzer, 1978).

Appendix E: Water Balance Residuals

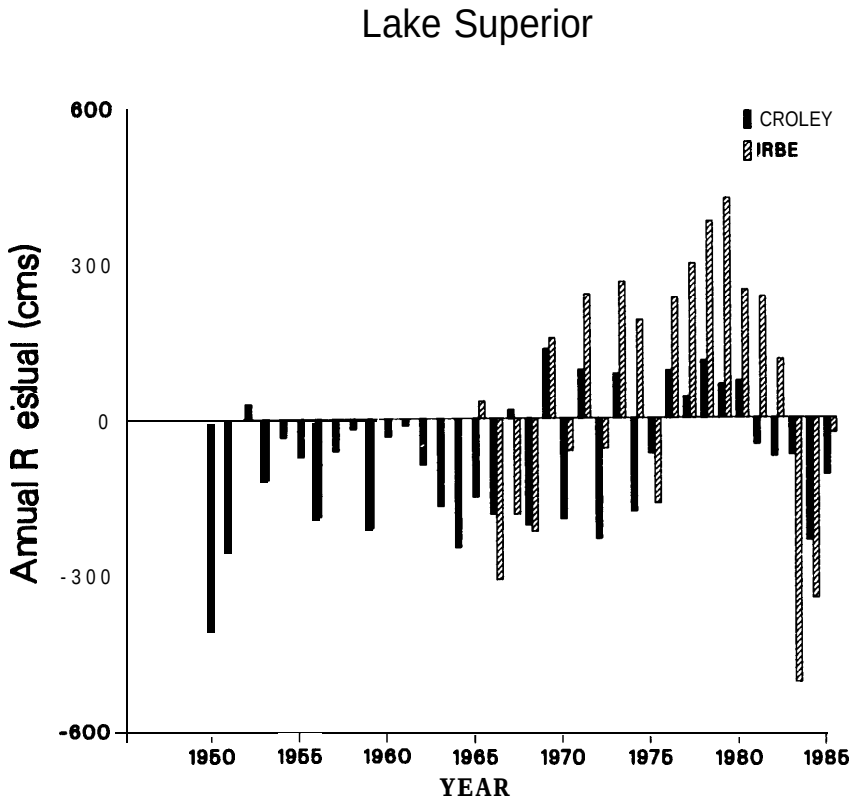

Figure E.1.--Lake Superior annual water balance residuals.

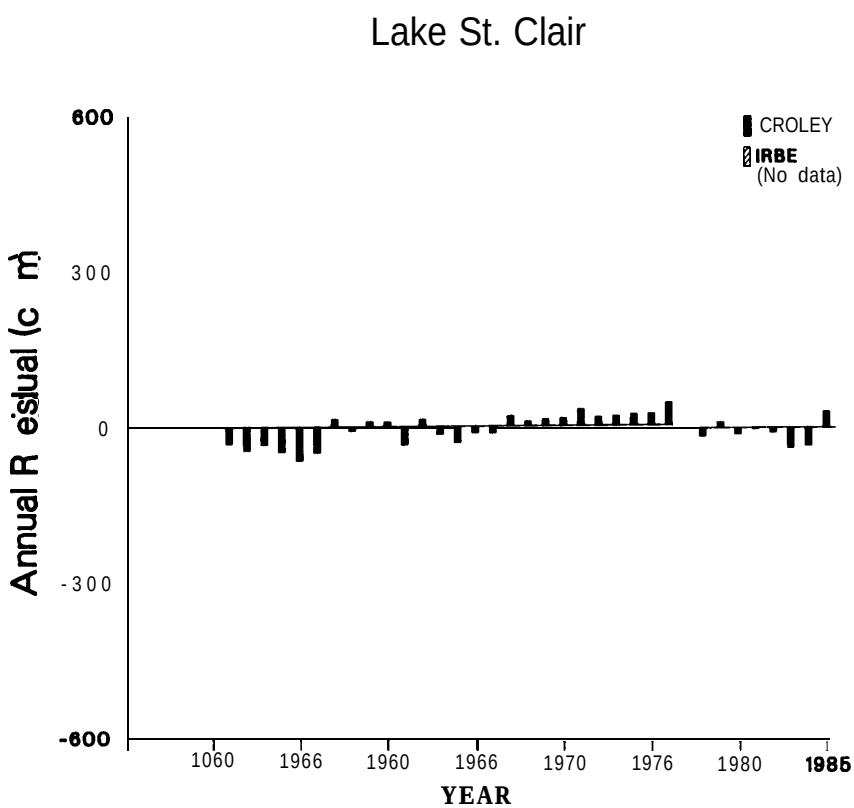

Figure E.2.--Lake St. Clair annual water balance residuals.

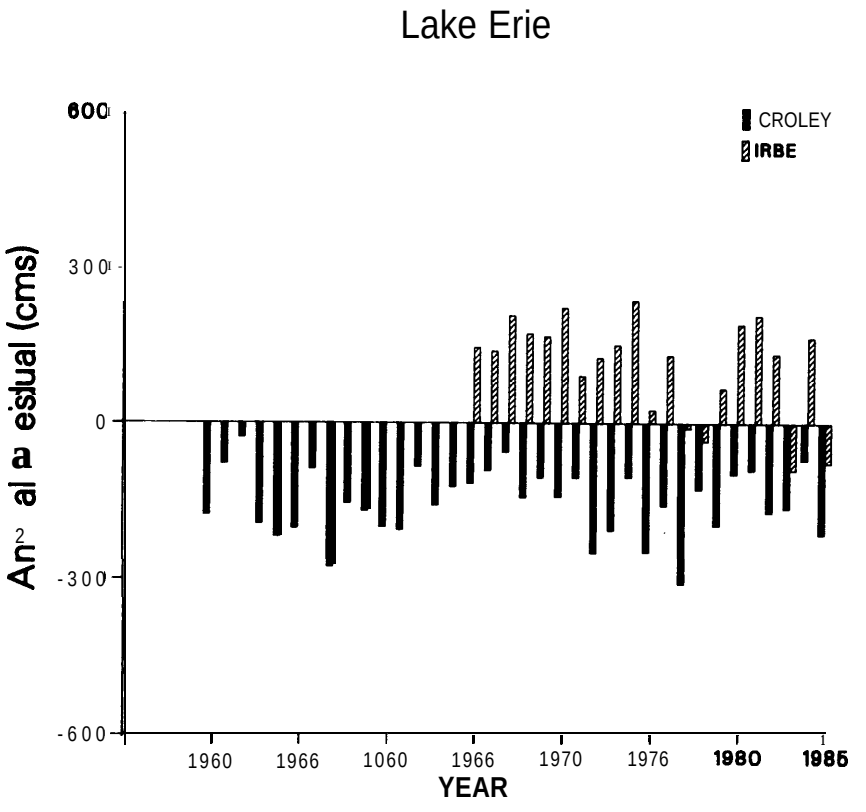

Figure E.3.–Lake Erie annual water balance residuals.

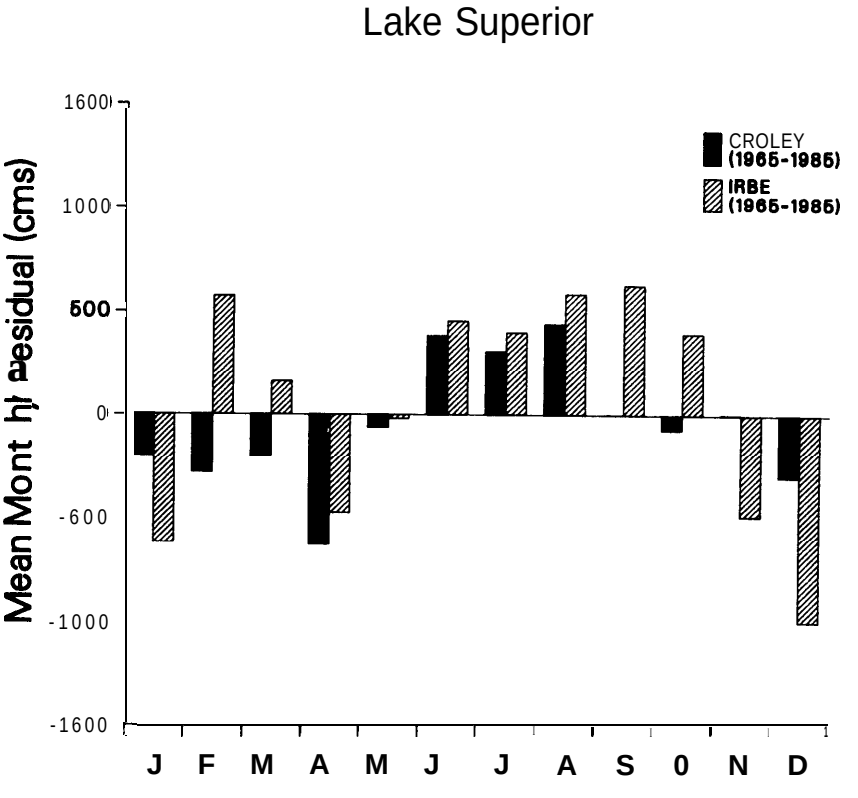

Figure E.4.--Lake Superior mean monthly water balance residuals.

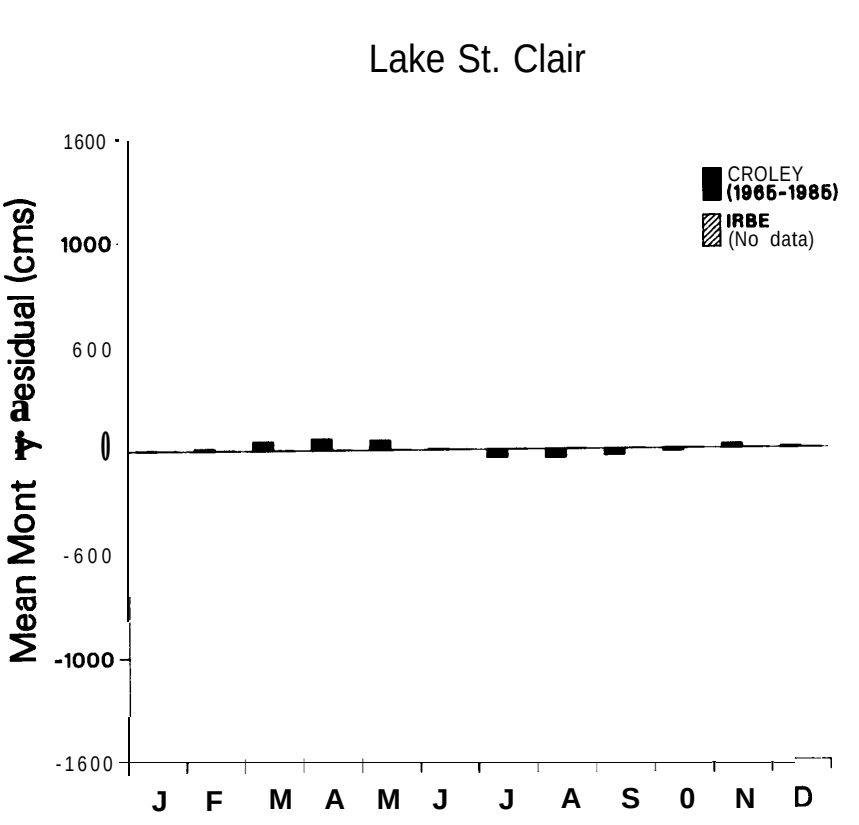

Figure E.5.--Lake St. Clair mean monthly water balance residuals.

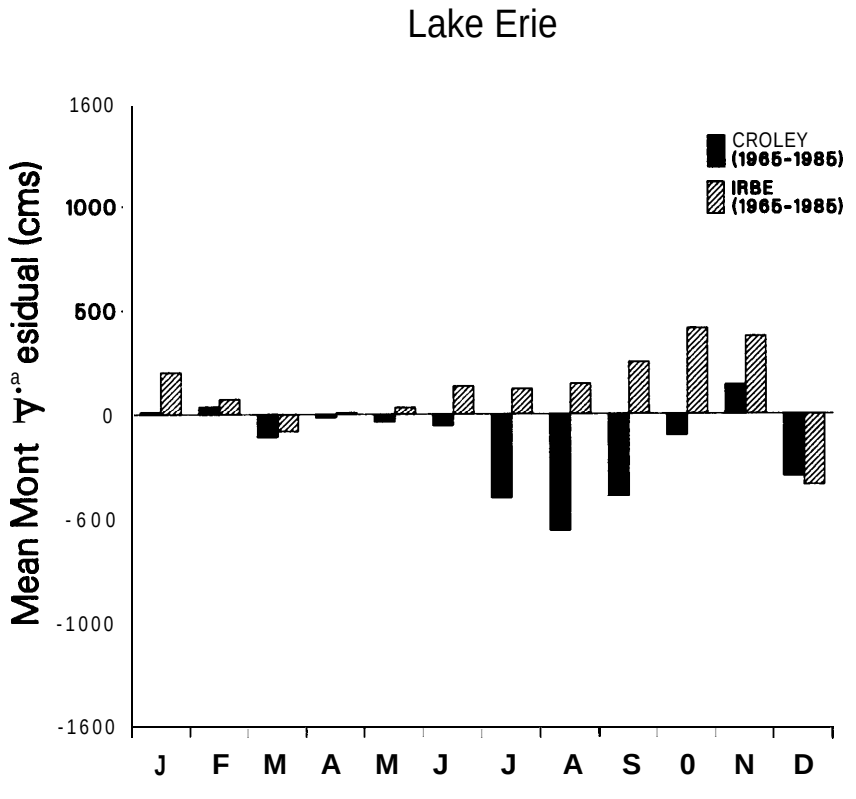

Figure E.G.--Lake Erie mean monthly water balance residuals.

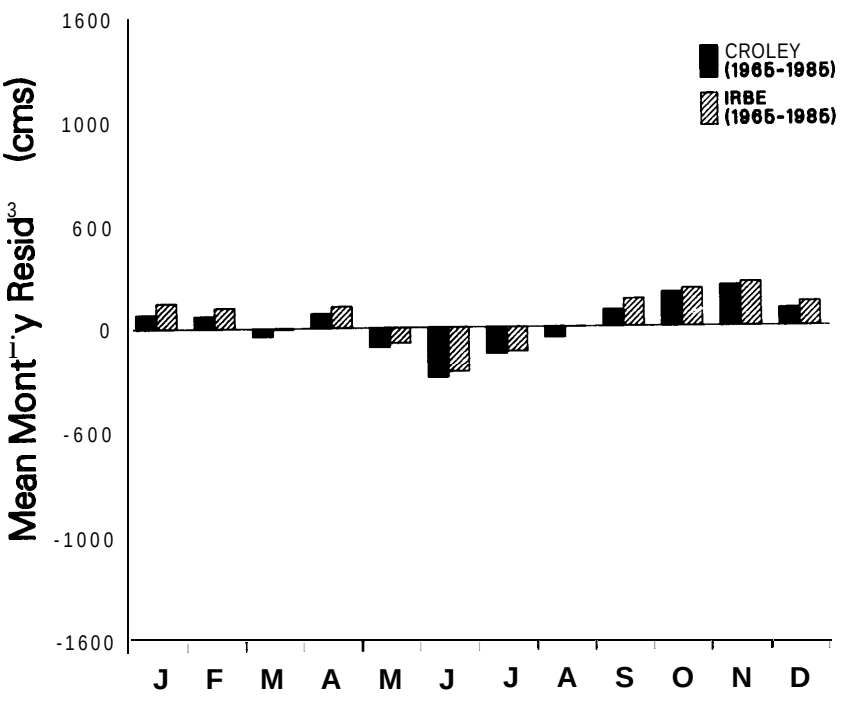

Figure E.7.--Lake Ontario mean monthly water balance residuals.

☆U.S. GOVERNMENT PRINTING OFFICE: 1989-656-486/80173